

000 001 002 003 004 005 006 007 008 009 010 011 012 013 014 015 016 017 018 019 020 021 022 023 024 025 026 027 028 029 030 031 032 033 034 035 036 037 038 039 040 041 042 043 044 045 046 047 048 049 050 051 052 053 TOPOLOGY OF ATTENTION DETECTS HALLUCINATIONS IN CODE LLMs

Anonymous authors

Paper under double-blind review

ABSTRACT

While the AI-code assistant tools become widespread, automatic assessment of the correctness of the generated code becomes a significant challenge. Code LLMs are prone to hallucinations, which may lead to code that does not solve a required problem, or even to code with severe security vulnerabilities. In this paper, we propose a new approach to assessment of code correctness. Our solution is based on topological data analysis (TDA) of attention maps of code LLMs. We carry out experiments with two benchmarks – HumanEval, MBPP and 5 code LLMs: StarCoder2-7B, CodeLlama-7B, DeepSeek-Coder-6.7B, Qwen2.5-Coder-7B, Magicoder-S-DS-6.7B. The experimental results show that the proposed method is better than several baselines. Moreover, the trained classifiers are transferable between coding benchmarks.

1 INTRODUCTION

Large Language Models (LLMs) are now widespread and have great potential to transform natural language processing and artificial intelligence. As far as code generation is concerned, LLMs that are trained on large amounts of code are capable of generating human-level code for a plethora of simple problems and are expected to revolutionize software engineering. At the same time, code-generating LLMs are prone to hallucinations of various types. For example, syntactic and runtime errors prevent proper program execution, while logical errors lead to incorrect solution of the problem. In some cases, the generated code might contain security issues or robustness issues, such as a memory leak. While many definitions of hallucinations exist, in this paper we assume that code hallucination is a code which is not functionally correct, that is, does not pass functional tests. For a wide adoption of code LLMs, there is a high need for automatic assessment of code quality. Regarding the current state of technology, a significant amount of time is spent on debugging and automatic rewriting of generated code (Liang et al., 2024).

We hypothesize that code quality can be inferred before its execution from an internal state of LLM, in particular its attention maps. Previous studies have shown that transformer attention maps are useful for artificial text detection (Kushnareva et al., 2021), acceptability judgment (Cherniavskii et al., 2022) and speech classification (Tulchinskii et al., 2022).

Attention maps of LLMs are shown to capture semantically meaningful information and might be an illustration of the model’s “thinking process”. The research community actively studies approaches to mitigate hallucinations of LLMs by external knowledge bases (Peng et al., 2023) or to reduce them to some extent (Elaraby et al., 2023). It is highly desirable to evaluate the quality of the code before its execution and a run of tests since the code might contain security vulnerabilities.

The study of hallucinations in LLMs is intrinsically tied to generalization in NLP models. Both challenges stem from the way models learn, represent, and apply knowledge. Improving generalization through robust training, diverse data, and better uncertainty handling reduces hallucinations by ensuring that the models produce contextually appropriate and factually grounded output. In contrast, analyzing hallucinations provides an insight into generalization failures, guiding the development of more reliable NLP systems. This symbiotic relationship underscores the importance of addressing both issues holistically in AI research.

Out contributions are the following:

054

- We propose a new approach to detection of hallucinations in LLM-generated code based
- 055 on analyzing a topology of attention maps;
- 056
- We carry out computational experiments with CodeLlama, StarCoder2, DeepSeek-Coder
- 057 and Qwen2.5-Coder and two benchmarks – HumanEval and MBPP, and show that the
- 058 proposed method outperforms baselines;
- 059
- We empirically show that the proposed hallucination classifier is transferable between code
- 060 benchmarks.
- 061

062

2 RELATED WORK

063

064

Code generation via LLMs is a topic of active research. The popular projects are CodeLlama (Roziere et al., 2023), StarCoder2 (Lozhkov et al., 2024), DeepSeek-Coder (Guo et al., 2024), Qwen2.5-Coder (Hui et al., 2024), to name a few. Code LLMs differ by the data used for training, by their training and fine-tuning protocols, including RLHF, tokenizers, variants of attention mechanism, etc.

065

Several works studied attention maps in transformer-based LLMs. Clark et al. (2019) studied BERT’s attention patterns: attending to delimiter tokens, specific positional offsets, or broadly attending over the whole sentence, with heads in the same layer often exhibiting similar behaviors. Clark et al. (2019) further showed that certain attention heads correspond well to the linguistic notions of syntax and coreference. Htut et al. (2019) found that for some universal dependency tree relation types, there exist heads that can recover the dependency type significantly better than baselines on parsed English text, suggesting that some self-attention heads act as a proxy for syntactic structure. Michel et al. (2019) showed that for downstream tasks, a large proportion of attention heads can be removed at test time without significantly affecting performance and that some layers can even be reduced to a single head.

066

The phenomenon of code hallucinations is studied and categorized in several papers. Tian et al. (2024) introduces a categorization of code hallucinations into four main types: mapping, naming, resource, and logic hallucinations, with each category further divided into different subcategories. Tian et al. (2024) proposed the CodeHalu dataset and studied the frequencies of different types of hallucinations in popular code LLMs. Liu et al. (2024) categorized hallucinations as intent conflicting, inconsistency, repetition, knowledge conflicting, dead code. Liu et al. (2024) released a HaluCode benchmark with code hallucinations labeled. Jiang et al. (2024) proposed Collu-Bench, the benchmark with localized code hallucinations. Jiang et al. (2024) found that code LLMs are less confident when hallucinating, since hallucinated tokens have a lower probability and hallucinated generation steps have a higher entropy. **Tong & Zhang (2024) proposed to guide an LMM to work in the “slow thinking” regime to obtain a more accurate evaluation of generated code correctness.**

067

In the broader context of NLP, several works introduced methods for preventing and detecting hallucinations. Peng et al. (2023) proposed to mitigate hallucination with an LLM-AUGMENTER, a system that allows the LLM to generate responses grounded in external knowledge, for example, stored in task-specific databases. Zhang et al. (2024b) proposed Self-Eval, a self-evaluation component, to prompt an LLM to validate the factuality of its own generated responses solely based on its internal knowledge. Feng et al. (2024) proposed two novel approaches for hallucination detection that are based on model collaboration, i.e., LLMs that investigate other LLMs for knowledge gaps, cooperatively or competitively. Zhang et al. (2024a) proposed to improve the truthfulness of LLMs by editing their internal representation during inference in the “truthful” space. Yehuda et al. (2024) introduced InterrogateLLM, a method that prompts the model multiple times to reconstruct the input query using the generated answer. Subsequently, InterrogateLLM quantifies the level of inconsistency between the original query and the reconstructed queries.

068

3 BACKGROUND

069

070

3.1 TRANSFORMER-BASED LLMs

071

072

All state-of-the art code LLMs are based on different variants of the transformer architecture (Vaswani, 2017).

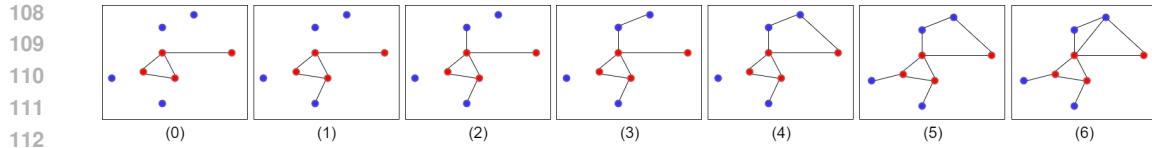


Figure 1: An example of MTD evaluation for a graph having two groups of vertices – red and blue. (0): initially, only edges connecting red vertices are present. (1)-(6): the rest of edges are added sequentially in an ascending order by their weights. While adding edges, connected components merge with each other. These moments are depicted by H_0 bars in Fig. 2. At moment (4) a cycle appears, at moment (6) this cycle disappears. These moments are depicted by the H_1 bar in Fig. 2.

A transformer architecture comprises L layers of multi-head self-attention blocks, each of them having H heads. Each attention head takes the matrix $X \in \mathbb{R}^{n \times d}$ as an input, and an output is $X^{out} = A(XW^V)$, where

$$A = \text{softmax} \left(\frac{(XW^Q)(XW^K)^T}{\sqrt{d}} \right),$$

and $W^Q, W^K, W^V \in \mathbb{R}^{d \times d}$ are projection matrices, and $A \in [0, 1]^{n \times n}$ is an **attention map**. In the self-attention block, the attention map shows how each token in the input sequence “interacts” with every other token in the same sequence. A token might attend more to other tokens that are contextually related. We interpret each element $a_{i,j}$ of an attention map as an “interaction force” between tokens i and j .

3.2 REPRESENTING AN ATTENTION MAP BY A WEIGHTED GRAPH

While attention map is typically presented as a matrix, we treat it as a weighted graph. For n tokens in a sequence, we consider a fully-connected weighted graph with n vertices, where weights of edges are related to the “interaction force” between tokens (vertices). The natural idea is to leave only the most interacting tokens, that is, attending to each other higher than some threshold. However, the optimal threshold is not known in advance. Moreover, the topology of such a graph changes discontinuously with the change of a threshold (or weights). Topological Data Analysis (TDA) (Chazal & Michel, 2017) introduces a principled way to access the topology of such graphs for all thresholds simultaneously.

3.3 MANIFOLD TOPOLOGY DIVERGENCE

MTD (Manifold Topology Divergence) (Barannikov et al., 2021) is a tool of TDA that can be used to evaluate the “dissimilarity” between two sets of vertices in a weighted graph $\mathcal{G} = (V, E, W)$ or, in other words, to which degree one set of vertices is covered by another set.

Let a set of vertices $V = P \sqcup G$, be split into disjoint sets P, G . We consider a nested sequence of graphs $\mathcal{G}_0 \subset \dots \subset \mathcal{G}_i \subset \mathcal{G}_{i+1} \subset \dots \subset \mathcal{G}$ in the following way. \mathcal{G}_0 has all the vertices P, G and all the edges that connect the vertices of P . The sequence \mathcal{G}_i is obtained by adding the rest of the edges one by one in ascending order of their weights; see Figure 1. During this process, graph topology naturally changes: connected components are merged, cycles appear and disappear, etc. This process is rigorously described by the theory of *persistence barcodes* (Chazal & Michel, 2017). Each topological feature, such as connected component or cycle, has a “birth time” and a “death time”, by a corresponding edge weight. The multi-set of these birth-death pairs (intervals) altogether is called a *Cross-Barcode*, see Figure 2. Here k is an index of a *persistence homology*, each of them reflects a kind of topological feature: 0 - connected components, 1 - cycles, 2 - voids, etc. MTD_k is an integral characteristic of a *Cross-Barcode* and it is defined as a sum of birth-death intervals’ lengths. The higher MTD_k is, the greater is the “dissimilarity” between sets of tokens. Note that according to a definition, MTD_k is not symmetric. Also, MTD_k , as a kind of persistence barcode, enjoys stability w.r.t. small perturbations of weights (Cohen-Steiner et al., 2005).

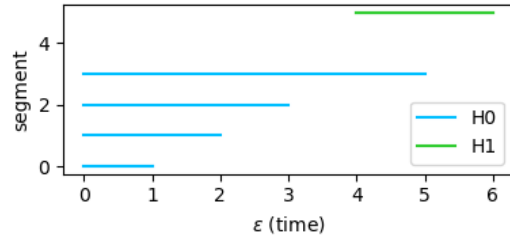


Figure 2: Cross-Barcode for a filtration from Fig. 1.

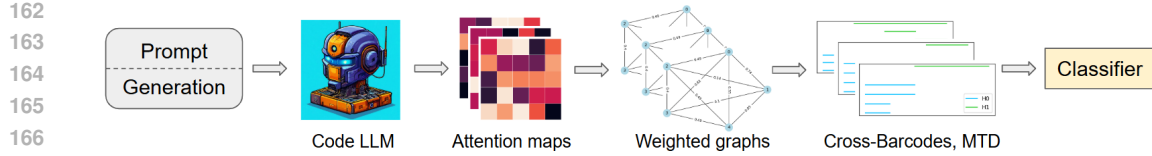


Figure 3: A pipeline of the proposed method for hallucination detection: (1) a prompt concatenated with a generated code is fed into a Code LLM. (2) Attention maps from the Code LLM are obtained. (3) Attention maps are transformed into fully-connected weighted graphs. (4) Cross-Barcodes and MTD features for weighted graphs are calculated. (5) On the top of the generated features a binary classifier of hallucinations is fitted.

Table 1: Characteristics of generated data: Pass@1, number of correct (#Pos.) and incorrect (#Neg.) solutions for each of the selected code LLMs.

Model	HumanEval			MBPP		
	Pass@1	#Pos.	#Neg.	Pass@1	#Pos.	#Neg.
StarCoder2-7B	28.9	1186	2914	42.8	1071	1429
CodeLlama-7B	25.9	1064	3036	35.2	879	1621
DeepSeek-Coder-6.7B	40.3	1653	2447	52.6	1315	1185
Qwen2.5-Coder-7B	47.8	1961	2139	52.1	1302	1198
Magicoder-S-DS-6.7B	65.5	2689	1411	61.3	1533	967

4 METHODS

In the context of code generation, we naturally have two sets of tokens – a prompt and a generation. A common cause of hallucination is when the model’s attention drifts away from the prompt¹. Our topology-based features quantify this mismatch, yet the same signal helps to identify other error patterns as shown below (Section 5.6). As was pointed out in Section 3.2, attention matrices can be analyzed as weighted graphs. Specifically, for n tokens in a sequence, we consider a fully-connected undirected weighted graph with n vertices, where weights of edges are obtained from an attention map: $w_{i,j} = 1 - a_{i,j}$, for $i > j$ (we used decoder-only LLMs with causal attention).

Then, Cross-Barcode and MTD for a weighted “attention graph” can be calculated². To predict code hallucinations, we use the following set of features:

- $MTD_0(P, G)/|G|$, $MTD_0(G, P)/|P|$
- $MTD_1(P, G)/|G|$, $MTD_1(G, P)/|P|$
- $\sum_{i \in P} a_{i,i}/|P|$, $\sum_{i \in G} a_{i,i}/|G|$

Here, all features are normalized by the size of the set of corresponding vertices for better transferability. In addition, sums of diagonal values of the attention matrices that are not directly present in edge weights are included. These features are calculated for every layer and head of a code LLM. At the top of the proposed topological features, we applied XGBoost (Chen & Guestrin, 2016) for a classification³. The high-level pipeline of the proposed method is shown in Figure 3.

MTD, when applied to attention graphs, measures the strength of connectivity between tokens of the generation and tokens of the prompt. Low values of MTD mean the high connectivity 1) between tokens of the generation and the prompt 2) between tokens inside the generation. MTD scores of some heads have a significant discriminative power and are shown in Fig. 4. Lack of generation-prompt attention means that representations of tokens from generation does not depend on prompt. That is, LLM drifts away from the prompt during generation and hallucinates.

¹The definition of hallucination is discussed in the Appendix G.

²Appendix D contains examples of Cross-Barcodes and corresponding attention maps.

³Appendix E contains an ablation study of a classifier model.

216

5 EXPERIMENTS

217

5.1 GENERATION OF DATASETS

218 To assess the efficacy of the proposed method for hallucination prediction, we carried out a set of
 219 computational experiments. In the main experiments, we use the following popular code LLMs:
 220 StarCoder2-7B (Lozhkov et al., 2024), CodeLlama-7B (Roziere et al., 2023), DeepSeek-Coder-
 221 6.7B (Guo et al., 2024), Qwen2.5-Coder-7B (Hui et al., 2024), Magicoder-S-DS-6.7B (Wei et al.,
 222 2024). We adapted two public benchmarks for evaluation of code generation: HumanEval (Chen
 223 et al., 2021) and MBPP (Austin et al., 2021)⁴. In order to account for various possible code gen-
 224 erations, for each of the coding problems, several solutions were generated by each of the selected
 225 code LLMs: we obtained 25 generations per task for HumanEval and 5 generations per task for
 226 MBPP unless otherwise specified. To address the quality of the proposed approach in different LLM
 227 prompting regimes, we used a 0-shot prompt for the HumanEval dataset and a 1-shot prompt for the
 228 MBPP dataset. To enable diversity of the generated solutions, a **temperature sampling** was done (see
 229 [Appendix L](#) for evaluation with greedy decoding.) Thus, we obtain 4100 samples for HumanEval
 230 and 2500 samples for MBPP for each code LLM (see [Appendix A](#) for further details). Table 1
 231 presents a summary of code solutions generated. The correctness of the code is evaluated via func-
 232 tional tests provided together with the coding benchmarks. Functional tests check that the function
 233 called with certain arguments has the corresponding output (examples are shown in Figures 6, 7 in
 234 the [Appendix A](#)). Incorrect code is considered a “hallucination”; prediction of code’s correctness is
 235 a binary classification problem. The pass@1 metric is slightly lower than reported in original papers,
 236 mostly because we have used sampling with non-zero temperature instead of greedy search. Be-
 237 fore moving further, note that there is a strong negative dependency between prompt and generation
 238 lengths and code quality; see Figure 8, 9. The longer the prompt (i.e. task description) and gen-
 239 eration (i.e. task solution) are, the lower is the probability of code’s correctness. This dependency
 240 is more pronounced for HumanEval than for MBPP, because MBPP employed more complicated
 241 1-shot prompts. These attributes are natural baselines for hallucination’s prediction.

242

5.2 ANALYZING METHOD’S CLASSIFICATION QUALITY

243 Using the generated data, we estimate the classification quality of the proposed approach. We ap-
 244 plied 5-fold stratified group cross-validation where different solutions of the same coding prob-
 245 lem belonged to the same group. In this way, training and testing were performed always at non-
 246 overlapping coding problems (prompts). The reported results are the mean and standard deviation
 247 estimated over the 5 folds.

248 As baselines for comparison, we used the XGBoost classifier trained on simple features: tokenized
 249 prompt length, tokenized generation length, and mean log. probability of generated tokens Chen
 250 et al. (2021). **We provide a comparison with Pylint⁵, a static code analysis tool for Python.** In
 251 addition, we trained a linear classification head on top of a frozen CodeT5-base encoder Wang et al.
 252 (2021). Furthermore, we have adapted Self-Eval Zhang et al. (2024b) and Interrogate-LLM Yehuda
 253 et al. (2024) to detect hallucinations in LLM-generated code and also utilized them as baselines.
 254 Finally, we utilize a combination of all features, i.e. tokenized prompt length, tokenized generation
 255 length, mean log. probability, and the proposed attention features, to train a classifier (we refer to
 256 it ‘All Feat.’ for brevity). Training details are provided in [Appendix B](#). Table 2 presents the main
 257 results. Table 12 in the [Appendix](#) presents the additional results for the 32 – 34B models.

258 In the majority of cases, the proposed classifier based on the features of the attention maps performed
 259 significantly better than the baselines and demonstrated stable results for all models and datasets as
 260 measured by the ROC-AUC score. Further analysis revealed that some features made a significant
 261 contribution to classification quality; see Figure 4. The use of additional features can both decrease
 262 and increase overall performance. Thus, we believe that the proposed attention features are strong
 263 enough to capture the most important information for code hallucination detection.

264 ⁴Licenses of pretrained models and benchmarks permit use for research purposes.

265 ⁵<https://www.pylint.org/>

270 Table 2: Quality of code hallucination detection for HumanEval and MBPP datasets. **Bold** and
 271 underline denote the first and second best results.

272 273 274 275 276 277 278 279 280 281 282 283 284 285 286 287 288 289 290 291 292 293 294 295 296 297 298 299 300 301 302 303 304 305 306 307 308 309 310 311 312 313 314 315 316 317 318 319 320 321	HumanEval		MBPP	
	ROC-AUC	F1-Score	ROC-AUC	F1-Score
StarCoder2-7B				
Prompt Len.	54.5 \pm 6.6	24.6 \pm 11.2	51.2 \pm 2.3	40.0 \pm 3.8
Gen. Len.	57.7 \pm 5.6	13.5 \pm 4.8	57.7 \pm 0.9	45.4 \pm 3.5
Mean Log. Prob.	70.9 \pm 1.3	32.4 \pm 4.8	62.0 \pm 2.0	47.5 \pm 3.4
Pylint	58.9 \pm 1.0	49.6 \pm 4.7	53.0 \pm 0.6	61.4 \pm 1.0
CodeT5-base ft.	70.1 \pm 7.1	33.3 \pm 10.1	58.5 \pm 3.5	43.3 \pm 9.0
Self-Eval	50.0 \pm 2.9	0.0 \pm 0.0	58.9 \pm 2.6	0.0 \pm 0.0
Interrogate-LLM	63.9 \pm 2.1	48.1 \pm 4.2	58.6 \pm 2.6	60.9 \pm 1.3
Attn. Feat. (ours)	<u>82.9 \pm 2.7</u>	<u>54.2 \pm 6.9</u>	81.9 \pm 2.4	<u>68.4 \pm 5.3</u>
All Feat.	83.7 \pm 4.1	57.5 \pm 7.9	81.8 \pm 2.1	68.7 \pm 5.1
CodeLlama-7B				
Prompt Len.	61.6 \pm 4.4	25.7 \pm 15.0	59.1 \pm 4.2	35.4 \pm 2.9
Gen. Len.	60.1 \pm 5.3	10.6 \pm 7.0	60.8 \pm 2.5	24.2 \pm 5.3
Mean Log. Prob.	64.1 \pm 2.0	25.4 \pm 6.2	61.0 \pm 3.7	27.2 \pm 1.5
Pylint	55.1 \pm 0.3	43.7 \pm 4.8	53.1 \pm 0.5	53.5 \pm 1.1
CodeT5-base ft.	74.5 \pm 6.3	43.6 \pm 13.2	61.7 \pm 3.0	19.1 \pm 7.1
Self-Eval	49.7 \pm 1.7	39.6 \pm 4.4	50.0 \pm 0.0	0.0 \pm 0.0
Interrogate-LLM	67.9 \pm 2.5	44.5 \pm 4.2	57.6 \pm 2.4	52.5 \pm 1.6
Attn. Feat. (ours)	<u>85.6 \pm 3.9</u>	<u>56.4 \pm 7.2</u>	<u>83.4 \pm 3.3</u>	<u>64.0 \pm 4.4</u>
All Feat.	85.7 \pm 3.8	57.9 \pm 9.7	83.8 \pm 2.0	65.2 \pm 4.3
DeepSeek-Coder-6.7B				
Prompt Len.	56.2 \pm 4.6	44.4 \pm 4.3	52.5 \pm 2.5	56.4 \pm 3.6
Gen. Len.	57.9 \pm 2.4	34.4 \pm 4.9	54.6 \pm 1.9	59.4 \pm 1.3
Mean Log. Prob.	69.8 \pm 2.5	51.1 \pm 3.4	61.0 \pm 1.9	62.3 \pm 1.6
Pylint	54.6 \pm 0.8	59.7 \pm 3.1	52.8 \pm 0.4	70.1 \pm 1.6
CodeT5-base ft.	69.1 \pm 4.2	52.6 \pm 6.5	55.7 \pm 3.0	64.8 \pm 2.7
Self-Eval	56.7 \pm 2.5	0.0 \pm 0.0	51.1 \pm 0.6	69.2 \pm 1.6
Interrogate-LLM	71.8 \pm 2.4	62.9 \pm 2.7	60.1 \pm 5.1	69.0 \pm 1.8
Attn. Feat. (ours)	85.6 \pm 2.8	<u>68.9 \pm 5.5</u>	<u>82.6 \pm 1.9</u>	<u>76.5 \pm 2.7</u>
All Feat.	85.4 \pm 2.7	69.3 \pm 5.3	83.1 \pm 1.2	77.0 \pm 1.3
Qwen2.5-Coder-7B				
Prompt Len.	54.3 \pm 8.7	51.0 \pm 5.7	51.8 \pm 3.6	56.2 \pm 4.4
Gen. Len.	57.6 \pm 3.6	48.9 \pm 5.1	55.6 \pm 2.1	59.7 \pm 4.8
Mean Log. Prob.	63.1 \pm 2.4	55.6 \pm 5.5	61.5 \pm 1.3	60.4 \pm 1.8
Pylint	64.1 \pm 2.2	<u>71.4 \pm 6.3</u>	62.0 \pm 2.5	74.1 \pm 0.8
CodeT5-base ft.	65.9 \pm 3.7	58.2 \pm 4.5	56.0 \pm 1.3	65.2 \pm 2.0
Self-Eval	73.8 \pm 1.6	75.6 \pm 3.8	66.6 \pm 2.3	76.0 \pm 1.3
Interrogate-LLM	60.1 \pm 3.7	65.7 \pm 5.1	55.0 \pm 1.8	<u>68.3 \pm 2.1</u>
Attn. Feat. (ours)	<u>81.7 \pm 2.8</u>	70.2 \pm 4.2	<u>82.2 \pm 2.2</u>	75.4 \pm 1.7
All Feat.	81.8 \pm 2.3	69.6 \pm 3.0	82.3 \pm 2.0	76.7 \pm 1.7
Magicoder-S-DS-6.7B				
Prompt Len.	57.3 \pm 5.4	70.4 \pm 7.0	54.0 \pm 2.6	69.2 \pm 3.0
Gen. Len.	52.5 \pm 2.1	76.3 \pm 2.6	52.3 \pm 2.1	71.4 \pm 2.4
Mean Log. Prob.	71.0 \pm 5.3	78.4 \pm 2.9	60.5 \pm 3.7	71.4 \pm 2.1
Pylint	52.7 \pm 1.3	80.0 \pm 3.3	52.0 \pm 0.8	76.7 \pm 2.4
CodeT5-base ft.	64.7 \pm 2.7	77.5 \pm 2.7	61.0 \pm 3.7	74.8 \pm 1.4
Self-Eval	44.3 \pm 3.2	79.1 \pm 3.1	49.2 \pm 1.4	75.5 \pm 2.4
Interrogate-LLM	65.3 \pm 2.1	79.6 \pm 3.1	59.0 \pm 7.1	76.1 \pm 2.1
Attn. Feat. (ours)	82.3 \pm 4.9	80.7 \pm 3.6	81.5 \pm 1.6	80.6 \pm 2.0
All Feat.	81.8 \pm 3.3	80.7 \pm 3.0	81.2 \pm 2.0	80.6 \pm 2.2

322 Moreover, the classifier detects various failure modes: SyntaxError, ZeroDivisionError, NameError,
 323 etc., across six categories (Section 5.6, Table 5), confirming that the approach generalizes beyond
 the prompt-insufficient attention failure mode.

324
325
326 Table 3: pass@1 scores for variants of ranking of code generations.
327
328
329
330
331
332

Model	HumanEval		MBPP	
	Random	Clf. Prob.	Random	Clf. Prob.
StarCoder2-7B	28.6 \pm 5.5	43.3 \pm 9.0	43.0 \pm 3.6	49.6 \pm 4.6
CodeLlama-7B	26.0 \pm 5.1	39.7 \pm 7.2	35.2 \pm 3.3	43.6 \pm 3.4
DeepSeek-Coder-6.7B	39.1 \pm 4.9	56.7 \pm 7.4	53.0 \pm 2.5	61.4 \pm 2.3
Qwen2.5-Coder-7B	51.8 \pm 8.0	64.0 \pm 7.3	52.6 \pm 3.6	62.0 \pm 2.4
Magicoder-S-DS-6.7B	72.5 \pm 10.0	74.3 \pm 6.1	61.4 \pm 3.4	64.8 \pm 2.1

333
334 Furthermore, we evaluated the proposed approach on Java (high resource), Go (medium resource),
335 Rust (low resource), and Lua (niche) programming languages of the HumanEval subdivision of the
336 MultiPL-E dataset Cassano et al. (2023). The proposed Attn. Feat. classifier can detect halluci-
337 nations even in low resource and niche languages, and there are several separate features that per-
338 form robust across the languages; see Tables 17, 19, 20. Furthermore, Table 16 demonstrates that the
339 proposed Attn. Feat. classifier has consistent quality when the linguistic complexity of the prompt
340 is increased. Finally, for additional comparison with zero-shot classification via larger LLMs, see
341 Appendix J.
342

343
344

5.3 ANALYZING METHOD'S RANKING QUALITY

345 Next, we assess the usefulness of the proposed code hallucination classifier for ranking of code
346 generations. For each problem, all generations were ranked according to the predicted probability
347 of correctness and one with the highest probability was selected. A baseline was random selection
348 of a code generation. The use of a classifier always leads to a significantly higher pass@1 score; see
349 Table 3. This result justifies that the proposed Att. Feat. classifiers can distinguish different levels
350 of code correctness among several candidate solutions to the same problem. Even for more recent
351 Qwen2.5-Coder-7B and Magicoder-S-DS-6.7B, pass@1 can still be further improved with the use
352 of Attn. Feat. classifier.
353

354
355

5.4 METHOD'S TRANSFERABILITY BETWEEN BENCHMARKS

356 We further study the transferability of the classifiers based on topological features. In this setting,
357 hallucination classifiers for a fixed code LLM were trained on data for one benchmark (HumanEval,
358 MBPP) and evaluated on another, then repeated vise versa. Table 4 shows the results: the proposed
359 classifiers are transferable, although performance is lower when training and testing is done on the
360 same benchmark. The proposed attention features achieve better transferability in 70% of cases,
361 as measured by ROC-AUC for both the HE \rightarrow MBPP and MBPP \rightarrow HE transfer. We relate the
362 changes in the classifiers' performance compared to results from Section 5.2 to differences in the
363 prompt structure: we use 0-shot prompt for HumanEval and 1-shot prompt for MBPP. Next, it is
364 possible to further improve transferability by combining the proposed attention features with the
365 mean log. probability of a generation. The combined classifier outperforms the Mean. Log. Prob.
366 baseline in 80% of cases. This indicates that these two approaches cover different aspects, and the
367 proposed attention features are indeed useful.
368

369 Next, we study cross-model transferability of classifiers. A classifier trained on DeepSeek-Coder-
370 6.7B is transferable to Magicoder-S-DS-6.7B and vice versa. But it is not the case for CodeLlama-
371 7B. The reason is that Magicoder-S-DS-6.7B is a fine-tuned DeepSeek-Coder-6.7B and a correspon-
372 dence between attention heads persists, see Appendix M.
373

374
375

5.5 ANALYZING FEATURE IMPORTANCE

376 In its base setup, the proposed approach requires computation of attention features from attention
377 maps for all layers and heads. However, we observed that the trained XGBoost classifier experienced
378 a natural sparsity with only about 25% meaningful features, as measured by the feature importance
379 attributed by the classifier. To further explore the importance and selection of features, we followed

378 Table 4: Transferability of code hallucination detectors. Each classifier was trained on HumanEval
 379 (MBPP) dataset and tested on MBPP (HumanEval) dataset.

381 Model	382 HumanEval → MBPP		383 MBPP → HumanEval	
	384 ROC-AUC	385 F1-Score	386 ROC-AUC	387 F1-Score
388 StarCoder2-7B				
Prompt Len.	48.6	0.0	52.1	<u>45.0</u>
Gen. Len.	56.0	14.6	52.4	38.3
Mean Log. Prob.	63.7	36.2	71.8	45.4
CodeT5-base ft.	53.7	0.0	59.1	0.0
Attn. Features	<u>67.5</u>	0.14	<u>67.2</u>	25.5
Attn. Feat. (ours) + Mean. Log. Prob	71.0	<u>24.0</u>	61.7	15.7
390 CodeLlama-7B				
Prompt Len.	51.7	0.0	53.4	42.9
Gen. Len.	61.5	4.2	50.0	41.0
Mean Log. Prob.	57.7	15.2	65.0	<u>34.9</u>
CodeT5-base ft.	54.9	0.0	62.4	0.0
Attn. Features	<u>69.5</u>	0.2	80.3	34.1
Attn. Feat. (ours) + Mean. Log. Prob.	72.3	<u>15.1</u>	79.0	<u>34.9</u>
396 DeepSeek-Coder-6.7B				
Prompt Len.	48.0	15.6	52.2	<u>58.2</u>
Gen. Len.	55.3	41.4	54.0	51.3
Mean Log. Prob.	62.5	56.3	69.1	58.3
CodeT5-base ft.	53.4	0.0	55.9	57.4
Attn. Features	<u>67.7</u>	<u>70.4</u>	<u>72.4</u>	20.4
Attn. Feat. (ours) + Mean. Log. Prob.	68.0	71.0	72.5	22.6
403 Qwen2.5-Coder-7B				
Prompt Len.	49.9	34.1	51.1	<u>64.1</u>
Gen. Len.	51.6	46.1	54.5	54.3
Mean Log. Prob.	60.3	<u>60.4</u>	<u>64.7</u>	<u>60.8</u>
CodeT5-base ft.	49.1	52.3	51.6	65.6
Attn. Features	70.6	63.3	64.2	54.3
Attn. Feat. (ours) + Mean. Log. Prob.	<u>70.0</u>	55.7	65.4	56.1
409 Magicoder-S-DS-6.7B				
Prompt Len.	48.1	56.3	54.5	79.5
Gen. Len.	54.8	75.2	56.1	74.6
Mean Log. Prob.	63.7	74.9	69.8	76.5
CodeT5-base ft.	49.3	76.0	45.9	<u>79.2</u>
Attn. Features	73.5	<u>78.4</u>	56.9	37.6
Attn. Feat. (ours) + Mean. Log. Prob.	<u>71.8</u>	79.1	<u>63.7</u>	45.8

417 the two-stage pipeline. First, for a given sparsity level, we selected the most important features as
 418 measured by the feature importance attributed by the classifier trained on all attention features si-
 419 multaneously. Second, we trained a new XGBoost classifier on the selected set of attention features.
 420 As indicated by Figures 5, 10, the proposed feature selection procedure could retain only 5% of all
 421 attention features without a significant loss of classification quality, highlighting that only a limited
 422 number of all attention heads are relevant for hallucination detection.

423 We carry out additional experiments benchmarking different programming languages (Python, Go,
 424 Rust, Java) and find that topological features of some heads exhibit a high predictive performance
 425 consistently across all programming languages; see the Appendix K.

428 5.6 A FINE-GRAINED CLASSIFICATION OF ERROR TYPES

430 We carried out additional experiments to study the ability of the proposed approach to detect specific
 431 types of hallucinations. An exception in Python can be considered as a hallucination type. Here are
 the common exceptions from the HumanEval and MBPP benchmarks: *AssertionError*, *AttributeEr-*

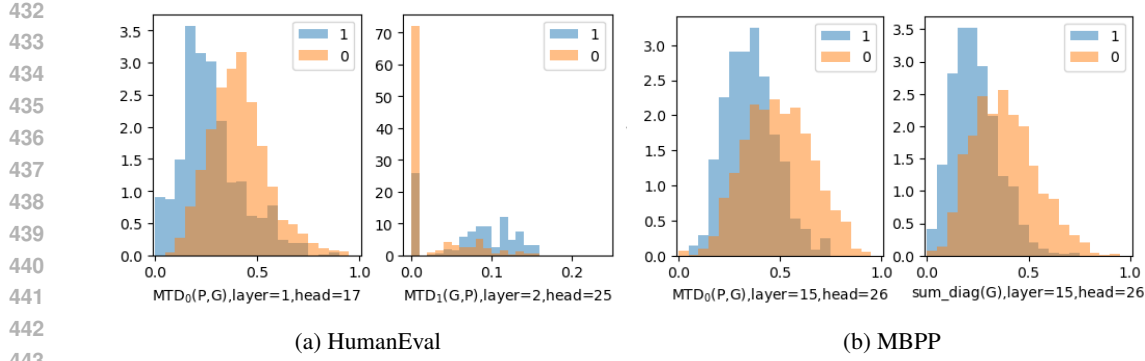


Figure 4: Distribution of classes (0-code is not correct, hallucination, 1-code is correct) vs. features from attention maps. Some of the most discriminative features are presented. Features are normalized with MinMaxScaler. Features come from CodeLlama-7B.

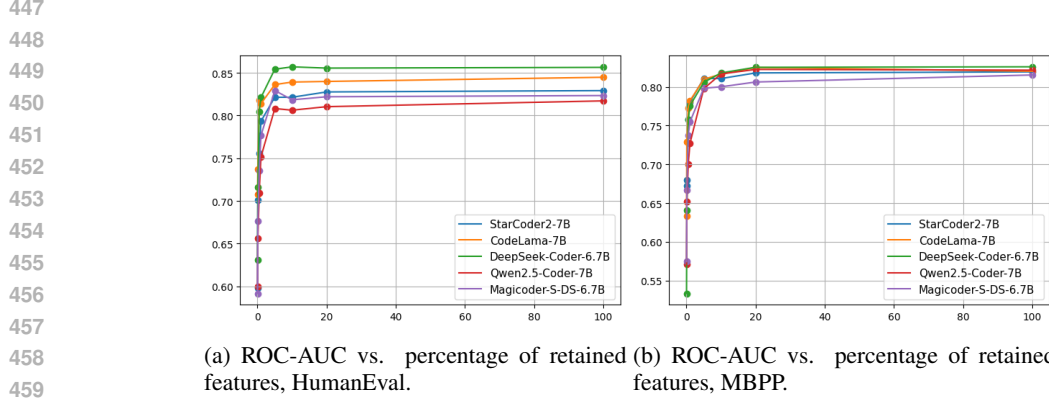


Figure 5: Analysis of feature importance of the proposed method, ROC-AUC.

rror, IndentationError, IndexError, ModuleNotFoundError, NameError, RecursionError, SyntaxError, TypeError, UnboundLocalError, ValueError, ZeroDivisionError, timed out

Therefore, we did multi-classification instead of binary classification in XGBoost. Table 5 shows the results. **This result demonstrates that the proposed attention features are capable of identifying the majority of errors of different types, consistently across the models.** Here is a breakdown of detection accuracy of particular types of errors for CodeLlama-7B: Assertion: 82.0%, IndexError: 97.8%, NameError: 75.7%, RecursionError: 100%, SyntaxError: 93.3%, TypeError: 80.6%, ValueError: 87.5%, ModuleNotFoundError, ZeroDivisionError, UnboundLocalError, IndentationError, AttributeError, timed out : 80%. Some error types were grouped because of a very low frequency.

5.7 ABLATION STUDY

The proposed approach is based on the two types of attention features: the diagonal elements of attention maps corresponding to a prompt and a generation, and topological features (MTD) computed for the corresponding “attention graph” (see Section 4 for details). In this Section, we provide an ablation study to estimate the contribution of each type of attention features. For this purpose, we trained the XGBoost classifier using 1) only MTD features, 2) only diagonal attention values, and 3) both types of features (our initial setup). As demonstrated in Table 9 in the Appendix, DeepSeek-Coder-6.7B and Qwen2.5-Coder-7B achieved the best performance when both types of attention features were used for HumanEval and MBPP datasets. In contrast, the best performance of StarCoder2-7B and Magicoder-S-DS-6.7B was achieved with different sets of attention features depending on the dataset and metric choices. In order to account for various information available via attention maps, we propose using both types of features as the most universal choice. Never-

486
487

Table 5: Performance of multi-classification of error types.

488

489

490

491

492

493

494

495

496

497

theless, we note that for some code LLM one certain type of attention features may result in better performance than combination of both types⁶.

498

499

500

6 CONCLUSIONS

In this paper, we propose a new hallucination detection approach for code-generating LLMs. Our approach is based on the introspection of an LLM: we get attention maps for a prompt and generation and study their topology after transforming to weighed graphs. The proposed topological features of these graphs have been empirically shown to be relevant for the detection of code hallucinations. A classifier built on top of these features outperformed several baselines. These classifiers are transferable across the coding benchmarks. The natural extension of our research is the detection of specific places of code with bugs, and we leave it for further research. We believe that our work may lead to a wider application of code LLMs by making them more reliable. In a wider context, our work contributes to the study of interpretation and generalization in NLP models, since hallucinations and generalization ability are intrinsically tied.

511

512

513

514

515

516

517

518

519

520

521

522

523

524

525

526

527

528

529

530

531

532

533

534

535

536

537

538

539

⁶Additional ablation study in Appendix I shows that for small models (QwenCoder-1.5b, QwenCoder-3b), and transfer learning setting, the differences in contribution of diagonal and MTD features is more pronounced.

540 **7 REPRODUCIBILITY STATEMENT**

541

542 The source code to reproduce the results presented is provided in the supplementary material. Hy-
 543 perparameters are either disclosed in the main text and Appendices A, B, or were equal to default
 544 values in the code.

546 **REFERENCES**

547

548 Jacob Austin, Augustus Odena, Maxwell Nye, Maarten Bosma, Henryk Michalewski, David Dohan,
 549 Ellen Jiang, Carrie Cai, Michael Terry, Quoc Le, et al. Program synthesis with large language
 550 models. *arXiv preprint arXiv:2108.07732*, 2021.

551 Serguei Barannikov, Ilya Trofimov, Grigorii Sotnikov, Ekaterina Trimbach, Alexander Ko-
 552 rotin, Alexander Filippov, and Evgeny Burnaev. Manifold topology divergence: a
 553 framework for comparing data manifolds. In Marc’Aurelio Ranzato, Alina Beygelz-
 554 imer, Yann N. Dauphin, Percy Liang, and Jennifer Wortman Vaughan (eds.), *Advances*
 555 in *Neural Information Processing Systems 34: Annual Conference on Neural Infor-*
 556 *mation Processing Systems 2021, NeurIPS 2021, December 6-14, 2021, virtual*, pp.
 557 7294–7305, 2021. URL <https://proceedings.neurips.cc/paper/2021/hash/3bc31a430954d8326605fc690ed22f4d-Abstract.html>.

558 Federico Cassano, John Gouwar, Daniel Nguyen, Sydney Nguyen, Luna Phipps-Costin, Donald
 559 Pinckney, Ming-Ho Yee, Yangtian Zi, Carolyn Jane Anderson, Molly Q Feldman, Arjun Guha,
 560 Michael Greenberg, and Abhinav Jangda. Multipl-e: A scalable and polyglot approach to bench-
 561 marking neural code generation. *IEEE Transactions on Software Engineering*, 49(7):3675–3691,
 562 2023. doi: 10.1109/TSE.2023.3267446.

563 Frédéric Chazal and Bertrand Michel. An introduction to topological data analysis: fundamental
 564 and practical aspects for data scientists. *CoRR*, abs/1710.04019, 2017.

565 Mark Chen, Jerry Tworek, Heewoo Jun, Qiming Yuan, Henrique Ponde De Oliveira Pinto, Jared
 566 Kaplan, Harri Edwards, Yuri Burda, Nicholas Joseph, Greg Brockman, et al. Evaluating large
 567 language models trained on code. *arXiv preprint arXiv:2107.03374*, 2021.

568 Tianqi Chen and Carlos Guestrin. Xgboost: A scalable tree boosting system. In *Proceedings of the*
 569 *22nd ACM SIGKDD international conference on knowledge discovery and data mining*, pp. 785–794,
 570 2016.

571 Daniil Cherniavskii, Eduard Tulchinskii, Vladislav Mikhailov, Irina Proskurina, Laida Kushnareva,
 572 Ekaterina Artemova, Serguei Barannikov, Irina Piontkovskaya, Dmitri Piontkovski, and Evgeny
 573 Burnaev. Acceptability judgements via examining the topology of attention maps. *arXiv preprint*
 574 *arXiv:2205.09630*, 2022.

575 Kevin Clark, Urvashi Khandelwal, Omer Levy, and Christopher D Manning. What does BERT look
 576 at? an analysis of BERT’s attention. *Proceedings of the 2019 ACL Workshop BlackboxNLP*, 2019.

577 David Cohen-Steiner, Herbert Edelsbrunner, and John Harer. Stability of persistence diagrams.
 578 In *Proceedings of the twenty-first annual symposium on Computational geometry*, pp. 263–271,
 579 2005.

580 Mohamed Elaraby, Mengyin Lu, Jacob Dunn, Xueying Zhang, Yu Wang, Shizhu Liu, Pingchuan
 581 Tian, Yuping Wang, and Yuxuan Wang. Halo: Estimation and reduction of hallucinations in
 582 open-source weak large language models. *arXiv preprint arXiv:2308.11764*, 2023.

583 Shangbin Feng, Weijia Shi, Yike Wang, Wenxuan Ding, Vidhisha Balachandran, and Yulia Tsvetkov.
 584 Don’t hallucinate, abstain: Identifying llm knowledge gaps via multi-llm collaboration. *arXiv*
 585 *preprint arXiv:2402.00367*, 2024.

586 Daya Guo, Qihao Zhu, Dejian Yang, Zhenda Xie, Kai Dong, Wentao Zhang, Guanting Chen, Xiao
 587 Bi, Yu Wu, YK Li, et al. Deepseek-coder: When the large language model meets programming—
 588 the rise of code intelligence. *arXiv preprint arXiv:2401.14196*, 2024.

594 Phu Mon Htut, Jason Phang, Shikha Bordia, and Samuel R Bowman. Do attention heads in bert
 595 track syntactic dependencies? *arXiv preprint arXiv:1911.12246*, 2019.
 596

597 Binyuan Hui, Jian Yang, Zeyu Cui, Jiaxi Yang, Dayiheng Liu, Lei Zhang, Tianyu Liu, Jiajun Zhang,
 598 Bowen Yu, Keming Lu, et al. Qwen2. 5-coder technical report. *arXiv preprint arXiv:2409.12186*,
 599 2024.

600 Nan Jiang, Qi Li, Lin Tan, and Tianyi Zhang. Collu-bench: A benchmark for predicting language
 601 model hallucinations in code. *arXiv preprint arXiv:2410.09997*, 2024.
 602

603 Laida Kushnareva, Daniil Cherniavskii, Vladislav Mikhailov, Ekaterina Artemova, Serguei Baran-
 604 nikov, Alexander Bernstein, Irina Piontovskaya, Dmitri Piontovski, and Evgeny Burnaev.
 605 Artificial text detection via examining the topology of attention maps. *arXiv preprint*
 606 *arXiv:2109.04825*, 2021.

607 Jenny T Liang, Chenyang Yang, and Brad A Myers. A large-scale survey on the usability of ai
 608 programming assistants: Successes and challenges. In *Proceedings of the 46th IEEE/ACM Inter-
 609 national Conference on Software Engineering*, pp. 1–13, 2024.
 610

611 Fang Liu, Yang Liu, Lin Shi, Houkun Huang, Ruijing Wang, Zhen Yang, Li Zhang, Zhongqi Li,
 612 and Yuchi Ma. Exploring and evaluating hallucinations in llm-powered code generation. *arXiv*
 613 *preprint arXiv:2404.00971*, 2024.

614 Anton Lozhkov, Raymond Li, Loubna Ben Allal, Federico Cassano, Joel Lamy-Poirier, Nouamane
 615 Tazi, Ao Tang, Dmytro Pykhtar, Jiawei Liu, Yuxiang Wei, et al. Starcoder 2 and the stack v2: The
 616 next generation. *arXiv preprint arXiv:2402.19173*, 2024.

617 Paul Michel, Omer Levy, and Graham Neubig. Are sixteen heads really better than one? *Advances*
 618 *in neural information processing systems*, 32, 2019.
 619

620 Baolin Peng, Michel Galley, Pengcheng He, Hao Cheng, Yujia Xie, Yu Hu, Qiuyuan Huang, Lars
 621 Liden, Zhou Yu, Weizhu Chen, et al. Check your facts and try again: Improving large language
 622 models with external knowledge and automated feedback. *arXiv preprint arXiv:2302.12813*,
 623 2023.

624 Baptiste Roziere, Jonas Gehring, Fabian Gloeckle, Sten Sootla, Itai Gat, Xiaoqing Ellen Tan, Yossi
 625 Adi, Jingyu Liu, Romain Sauvestre, Tal Remez, et al. Code llama: Open foundation models for
 626 code. *arXiv preprint arXiv:2308.12950*, 2023.

627 Yuchen Tian, Weixiang Yan, Qian Yang, Qian Chen, Wen Wang, Ziyang Luo, and Lei Ma.
 628 Codehalu: Code hallucinations in llms driven by execution-based verification. *arXiv preprint*
 629 *arXiv:2405.00253*, 2024.

630 Weixi Tong and Tianyi Zhang. Codejudge: Evaluating code generation with large language models.
 631 *arXiv preprint arXiv:2410.02184*, 2024.

632 Eduard Tulchinskii, Kristian Kuznetsov, Laida Kushnareva, Daniil Cherniavskii, Serguei Baran-
 633 nikov, Irina Piontovskaya, Sergey Nikolenko, and Evgeny Burnaev. Topological data analysis
 634 for speech processing. *arXiv preprint arXiv:2211.17223*, 2022.

635 A Vaswani. Attention is all you need. *Advances in Neural Information Processing Systems*, 2017.

636 Yue Wang, Weishi Wang, Shafiq Joty, and Steven C. H. Hoi. Codet5: Identifier-aware unified pre-
 637 trained encoder-decoder models for code understanding and generation, 2021. URL <https://arxiv.org/abs/2109.00859>.

638 Yuxiang Wei, Zhe Wang, Jiawei Liu, Yifeng Ding, and Lingming Zhang. Magicoder: Empowering
 639 code generation with OSS-instruct. In *Proceedings of the 41st International Conference on Ma-
 640 chine Learning*, volume 235 of *Proceedings of Machine Learning Research*, pp. 52632–52657.
 641 PMLR, 21–27 Jul 2024. URL <https://proceedings.mlr.press/v235/wei24h.html>.

648 Yakir Yehuda, Itzik Malkiel, Oren Barkan, Jonathan Weill, Royi Ronen, and Noam Koenigstein.
649 Interrogatellm: Zero-resource hallucination detection in llm-generated answers. In *Proceedings*
650 *of the 62nd Annual Meeting of the Association for Computational Linguistics (Volume 1: Long*
651 *Papers)*, pp. 9333–9347, 2024.

652 Shaolei Zhang, Tian Yu, and Yang Feng. Truthx: Alleviating hallucinations by editing large lan-
653 guage models in truthful space. *arXiv preprint arXiv:2402.17811*, 2024a.

654 Xiaoying Zhang, Baolin Peng, Ye Tian, Jingyan Zhou, Lifeng Jin, Linfeng Song, Haitao Mi, and
655 Helen Meng. Self-alignment for factuality: Mitigating hallucinations in llms via self-evaluation.
656 *arXiv preprint arXiv:2402.09267*, 2024b.

657
658
659
660
661
662
663
664
665
666
667
668
669
670
671
672
673
674
675
676
677
678
679
680
681
682
683
684
685
686
687
688
689
690
691
692
693
694
695
696
697
698
699
700
701

```

702
703     from typing import List
704
705     def has_close_elements(numbers: List[float], threshold: float) -> bool:
706         """ Check if in given list of numbers, are any two numbers closer to each other than
707         given threshold.
708         >>> has_close_elements([1.0, 2.0, 3.0], 0.5)
709         False
710         >>> has_close_elements([1.0, 2.8, 3.0, 4.0, 5.0, 2.0], 0.3)
711         True
712         """
713
714         for i in range(len(numbers) - 1):
715             for j in range(i+1, len(numbers)):
716                 if abs(numbers[i] - numbers[j]) <= threshold:
717                     return True
718
719         return False
720

```

Figure 6: Example of prompt (problem description) and model generation for the HumanEval dataset.

```

721     You are an expert Python programmer, and here is your task: Write a function to find the
722     similar elements from the given two tuple lists. Your code should pass these tests:
723
724     assert similar_elements((3, 4, 5, 6),(5, 7, 4, 10)) == (4, 5)
725     assert similar_elements((1, 2, 3, 4),(5, 4, 3, 7)) == (3, 4)
726     assert similar_elements((11, 12, 14, 13),(17, 15, 14, 13)) == (13, 14)
727     [BEGIN]
728     def similar_elements(test_tup1, test_tup2):
729         res = tuple(set(test_tup1) & set(test_tup2))
730         return (res)
731     [DONE]
732
733     You are an expert Python programmer, and here is your task: Write a python function to
734     remove first and last occurrence of a given character from the string. Your code should
735     pass these tests:
736
737     assert remove_Occ("hello","l") == "heo"
738     assert remove_Occ("abcpa","a") == "bcp"
739     assert remove_Occ("PHP","P") == "H"
740     [BEGIN]
741     def remove_Occ(s,c):
742         return s.replace(c,'',s.count(c)-1)
743     [DONE]
744

```

Figure 7: Example of prompt (one-shot example and problem description) and model generation for the MBPP dataset.

A DETAILS ON GENERATION PROCEDURE

We generate solutions for the coding problems with a temperature of 0.8. For the HumanEval dataset, the maximum length of the model output (i.e., input prompt + generation) was limited to 512 tokens. For the MBPP dataset, the maximum number of new tokens to generate was set to 256. Figures 6, 7 provide examples of prompts and generations for HumanEval and MBPP datasets. We followed the guidelines⁷ to post process the model output and extract the valid problem solution. To compute the attention features according to the method proposed in Section 4, we used the attention submatrix corresponding to the input prompt and the valid solution to the problem. For computational experiments, we used NVIDIA TITAN RTX.

⁷<https://github.com/bigcode-project/bigcode-evaluation-harness>

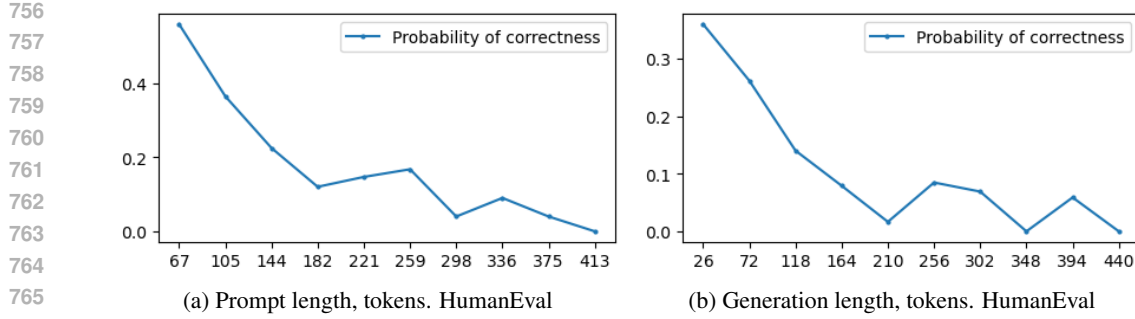


Figure 8: The individual conditional expectations for prompt and generation lengths, CodeLlama-7B.

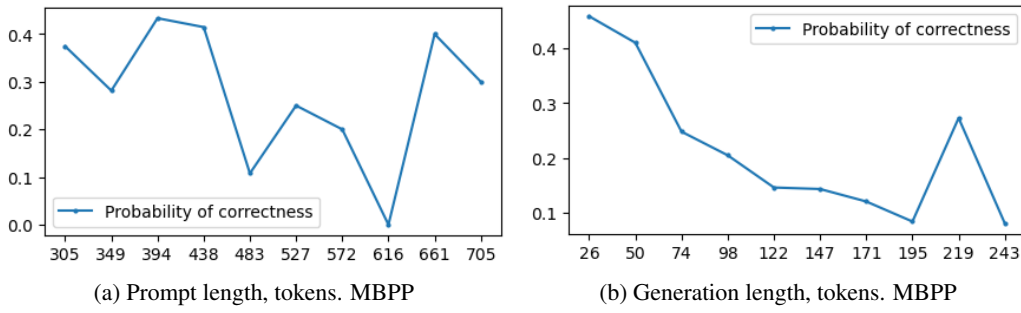


Figure 9: The individual conditional expectations for prompt and generation lengths, CodeLlama-7B.

B DETAILS ON TRAINING PROCEDURE

For the code hallucination detectors, based on the XGBoost classifier training, we utilized the XGB-Classifier with an approximation tree method “hist” from the XGBoost library⁸. For the code hallucination detector based on CodeT5-base embeddings, we used the pre-trained frozen CodeT5-base encoder with a trainable classification head consisting of 2 linear layers with hidden dimensionality 768. The classification head was trained for 100 epochs with batch size 32 and learning rate $3e - 5$.

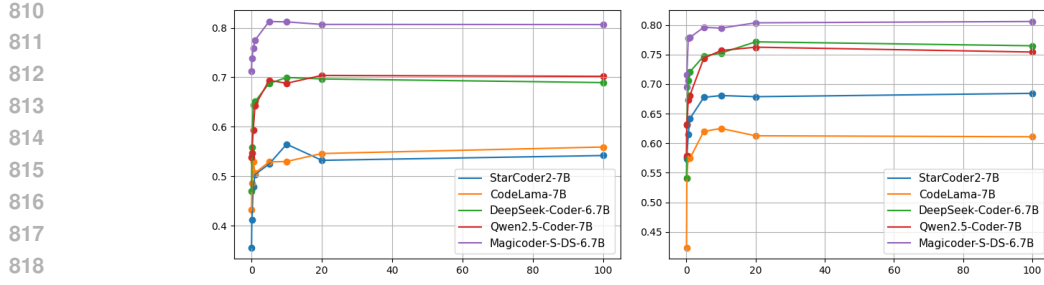
Self-Eval (Zhang et al., 2024b) is a way to evaluate the responses of an LLM using its internal knowledge. Self-Eval extracts a list of atomic claims from the responses and then prompts an LLM itself to validate the factuality of the claims. Self-Eval is not directly applicable to Code LLMs, since there are no “facts” in the code. However, we applied the core idea of Self-Eval by prompting Code LLMs to evaluate the functional correctness of a generated code. In addition, we have adapted Interrogate-LLM (Yehuda et al., 2024) to detect hallucinations in LLM-generated code. As an embedding model, we used the CodeT5+ 110M Embedding model, $K = 5$ and a fixed temperature.

C METRICS USED FOR EVALUATION

In order to account for possible class imbalance, we use ROC-AUC and F1-Score to evaluate the code hallucination detectors. We briefly introduce them in the following.

The ROC curve demonstrates the quality of a binary classifier for all possible classification thresholds. The X-axis corresponds to the False Positive Rate (FPR) and the Y-axis corresponds to the True Positive Rate (TPR) which can be defined as follows: $FPR = \frac{FP}{FP+TN}$, $TPR = \frac{TP}{TP+FN}$, where TP – true positive samples, FP – false positive samples, TN – true negative samples, FN –

⁸<https://xgboost.readthedocs.io/en/latest/index.html>



(a) F1 vs. percentage of retained features, (b) F1 vs. percentage of retained features, HumanEval. MBPP.

Figure 10: Analysis of feature importance of the proposed method, F1-score

false negative samples. ROC-AUC is defined as the area under the ROC curve. ROC-AUC of a random model is equal to 0.5, ROC-AUC of a perfect model is 1.

The F1-score is a harmonic mean of Precision and Recall:

$$F_1 = \frac{2}{\frac{1}{Precision} + \frac{1}{Recall}}.$$

To study the ranking ability of the hallucinations detector, we used the pass@1 metric. pass@1 is a proportion of coding problems from a benchmark for which a Code LLM generated the correct solution passing all the tests, with the restriction that only one solution (among 25 generations for HumanEval and 5 for MBPP) is executed.

D EXAMPLES OF CROSS-BARCODES

Figure 11 shows examples of Cross-Barcode₀ for a fixed attention head. The Cross-Barcode₁(P, G) is empty for these attention maps. Correct generations (a), (b) tend to have more and more H₀ bars than not-correct ones (c), (d).

Figure 12 shows examples of Cross-Barcode₀, Cross-Barcode₁ for a fixed attention head. Correct generations (a), (b) tend to have more and longer H₁ bars than not-correct ones (c), (d).

Attention maps for the corresponding head are shown in Figures 13, 14.

E EXPERIMENTS ON THE CLASSIFIER MODEL SELECTION

We carried out additional experiments with the feed-forward network (MLP), logistic regression, and support vector classifier (SVC) instead of XGBoost as a classifier for hallucination detection (the rightmost block in Figure 3). We used MLP with two hidden layers of size 256 and ReLU activations. This configuration was selected after moderate optimization of an architecture. For logistic regression and SVC, we tuned the value of regularization strength. Table 6 presents the results. MLP tends to have a lower ROC-AUC, but sometimes has a higher F1-score. While the F1-score is a threshold-dependent metric, the ROC-AUC integrates over all thresholds. In an unbalanced setting, ROC-AUC is often more stable, thus a classifier may have a higher ROC-AUC even when its F1-score is lower. XGBoost offers (a) strong average performance across all code LLMs, (b) negligible training cost (≈ 30 s per fold), and (c) no hyper-parameter tuning in our setting. XGBoost guarantees low computational overhead while providing a single, robust baseline for subsequent work.

F A NOTE ON APPLICABILITY OF GNNs TO ATTENTION MAPS

To train a GNN-based approach on graphs with edge weights obtained from attention matrices, these attention matrices need to be stored. We can estimate the approximate memory footprint to store

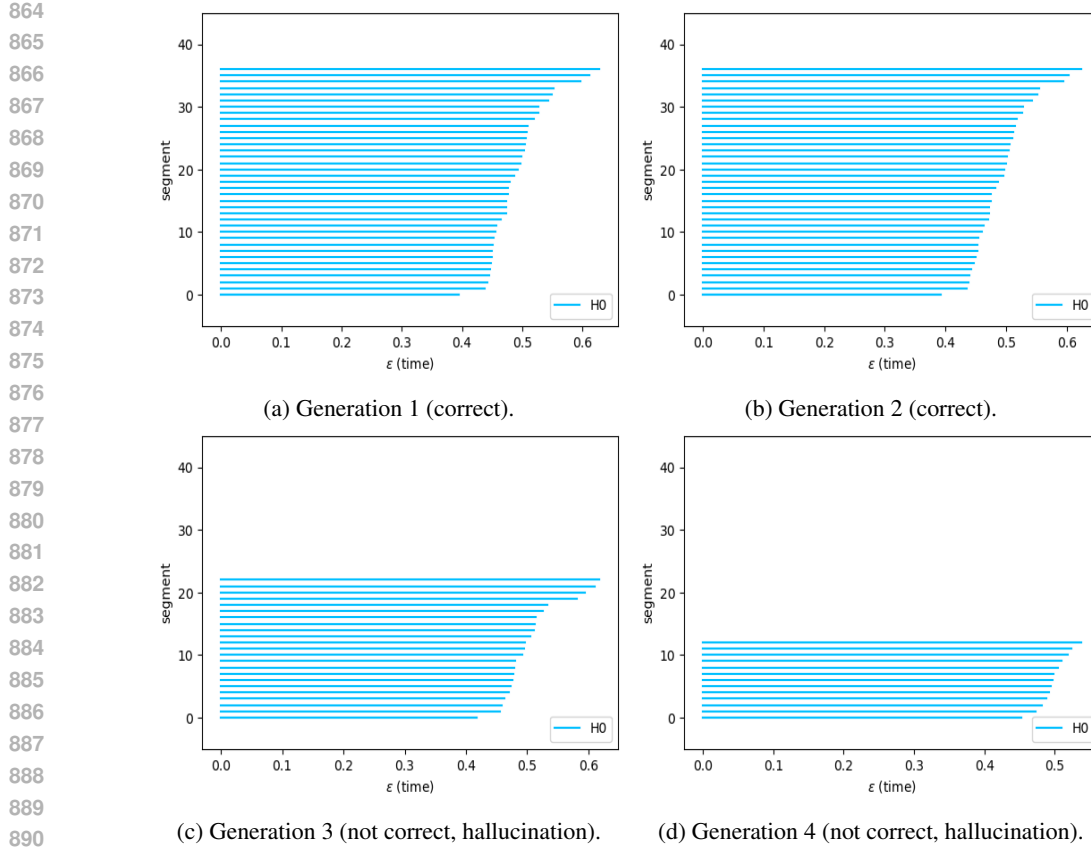


Figure 11: Examples of Cross-Barcode₀(P, G), CodeLLama-7B, HumanEval dataset, problem 14, layer 4, head 18. Cross-Barcode₁(P, G) is empty for these attention maps.

attention matrices of size $(\text{seq_len_k})^2$ for a model with n_layers and n_heads for a dataset of size N using the formula: $n_layers \times n_heads \times s \times \sum_{i=1}^k (\text{seq_len_k})^2$ where s is the size of the float type. We assume $s = 4$ bytes. If one uses only attention matrices from the last layer of the model, we obtain the memory footprint approximately 20.7 - 31.1 Gb for the Human Eval dataset and 36.6 - 53.7 Gb for MBPP (depending on the model). However, to store the attention matrices for all layers and all heads, the memory footprint is about 578.2 - 996.4 Gb for Human Eval and 1023.5 - 1718.7 Gb for MBPP. We highlight that even for datasets of moderate size (i.e. 4100 generations for HumanEval and 2500 generations for MBPP), the memory footprint becomes prohibitively high. Thus, it is not always feasible to store such features. In contrast, in our approach, we do not need to store the attention matrices since we compute all the features immediately during generation. Hence, the size of our training dataset is negligible.

We provide an estimate of computational time using the CodeLLama-7B model and HumanEval dataset as an example. The average time taken to generate a solution for one problem without feature extraction is 6.2 sec, with feature extraction 11.5 sec for all layers and heads, which are processed in parallel. Feature computation time during inference can be further decreased if only the most important features are used for classification: according to Section 5.5, it is possible to use only 5% of all attention features without significant loss of classification quality. The average memory footprint is ≈ 190 Mb for HumanEval and ≈ 544 Mb for MBPP. This size is a small fraction of GPU footprint during generation. Moreover, our approach demonstrates high performance without hyperparameter tuning. Therefore, we believe that the proposed approach has better scalability and is more practical.

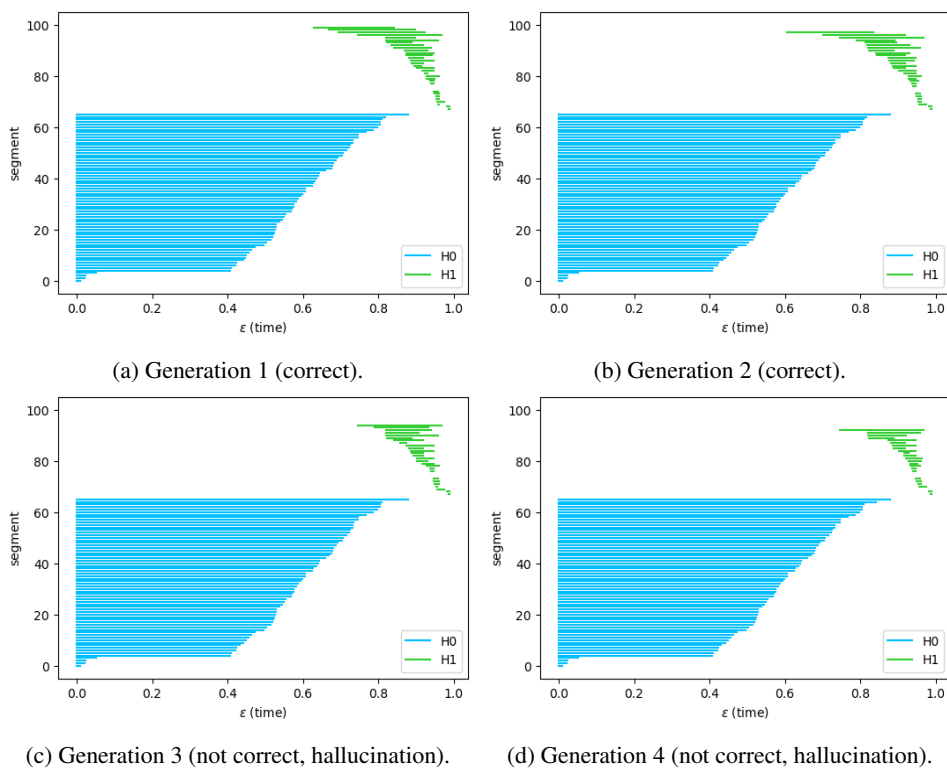


Figure 12: Examples of $\text{Cross-Barcode}_0(G, P)$, $\text{Cross-Barcode}_1(G, P)$. CodeLLama-7B, HumanEval dataset, problem 14, layer 15, head 5.

G ON DEFINITION OF A CODE HALLUCINATION

In our approach, the topological features obtained from attention maps account for the dissimilar structures in the prompt and generation subsets. Our intuition is that a correct solution should correspond to the structure of the prompt as their high-level semantic meanings correspond. Although other reasons behind hallucinations are possible, our approach estimates the correctness of code based only on the internal information flow of the model that does not require additional resources. Nevertheless, the proposed approach can be further integrated with other code hallucination detection tools to achieve better performance. Also, the most popular benchmarks like HumanEval and MBPP check only functional correctness, that is, whether a code solves the corresponding problem as stated in a prompt. Verification of a code is done by running functional tests, as explained in Section 5.1.

H LIMITATIONS

Although we have achieved good experimental results, we realize that our research has several limitations. Our method targets hallucinations that manifest in the geometry of the model’s attention; it does not unravel all root causes (e.g., spurious pre-training correlations, decoding drift, RLHF bias). Extending the analysis to these factors is left for future work. We mostly explored code LLMs that have no more than 7B parameters. Information in larger models is more distributed in attention heads and results might differ. Also, processing more attention heads is computationally costly. Next, the proposed classifiers for hallucination detection are based on the attention maps of the same code LLMs as for code generations. We leave a more general setting for further research. Finally, our approach can predict whether a code is correct as a whole but can not point to a specific place with a bug.

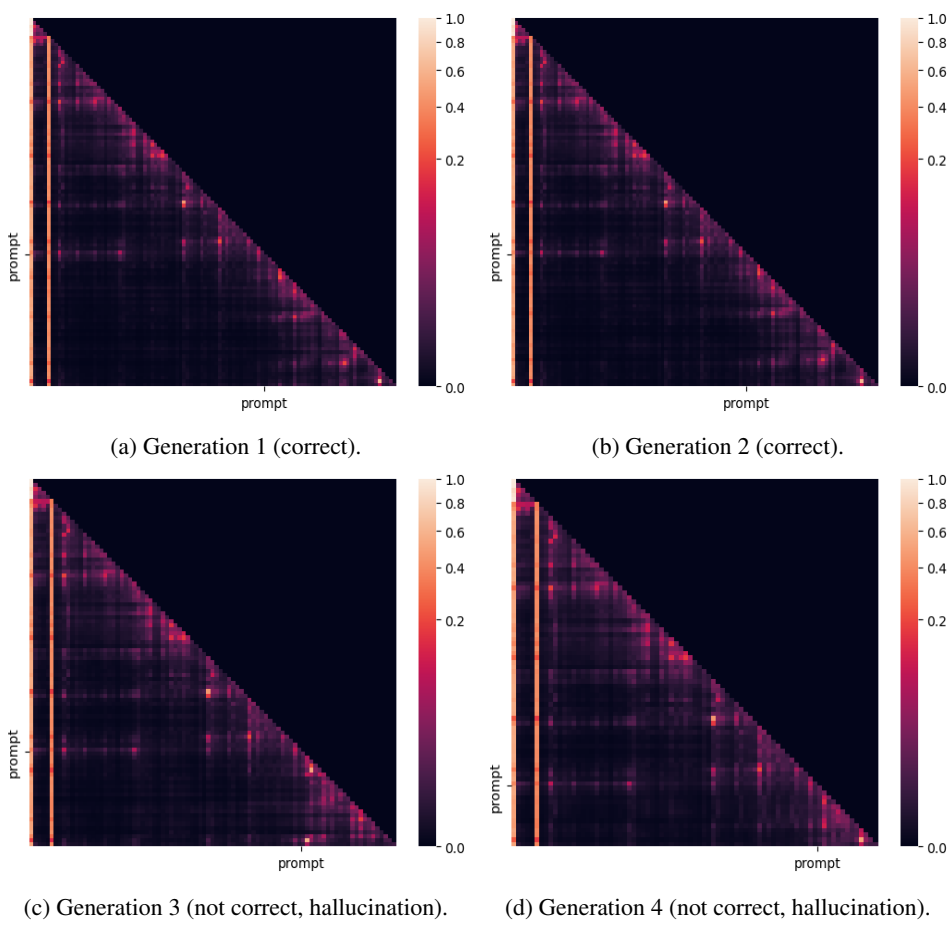


Figure 13: Attention maps. CodeLLama-7B, HumanEval dataset, problem 14, layer 4, head 18.

I ADDITIONAL ABLATION STUDY

Our main argument in the Ablation study is that different models benefit from different types of attention features. In this section, we provide an additional evaluation to further support our claim. We observe that the smaller QwenCoder-1.5b and QwenCoder-3b models experience a substantial performance decrease when topological features are removed; see Table 7. To further support our observations, we provide some examples of transferability from MBPP to HE datasets where the contribution of diagonal and MTD features is different for different models; see Table 8. Therefore, we propose to account for both types of features in our approach or at least to be aware of the potential benefits of using each type.

J EXPERIMENTS WITH LARGER MODELS

We carried out additional experiments, where code hallucinations are detected by a recent reasoning DeepSeek R1 model having 671 billion parameters with Chain of Thought inference on MBPP dataset. We used the following prompt:

You are provided with two coding tasks with solutions. The first one is just an example and does not need an assessment. Tell whether the second task is correctly solved by the code provided in the second [BEGIN] [DONE] block. The answer must be Yes or No

For code generated with the DeepSeek-6.7B model, we asked DeepSeek R1 using the above prompt, extracted the final answers (i.e. “Yes” or “No”) from the generated responses, and trained the

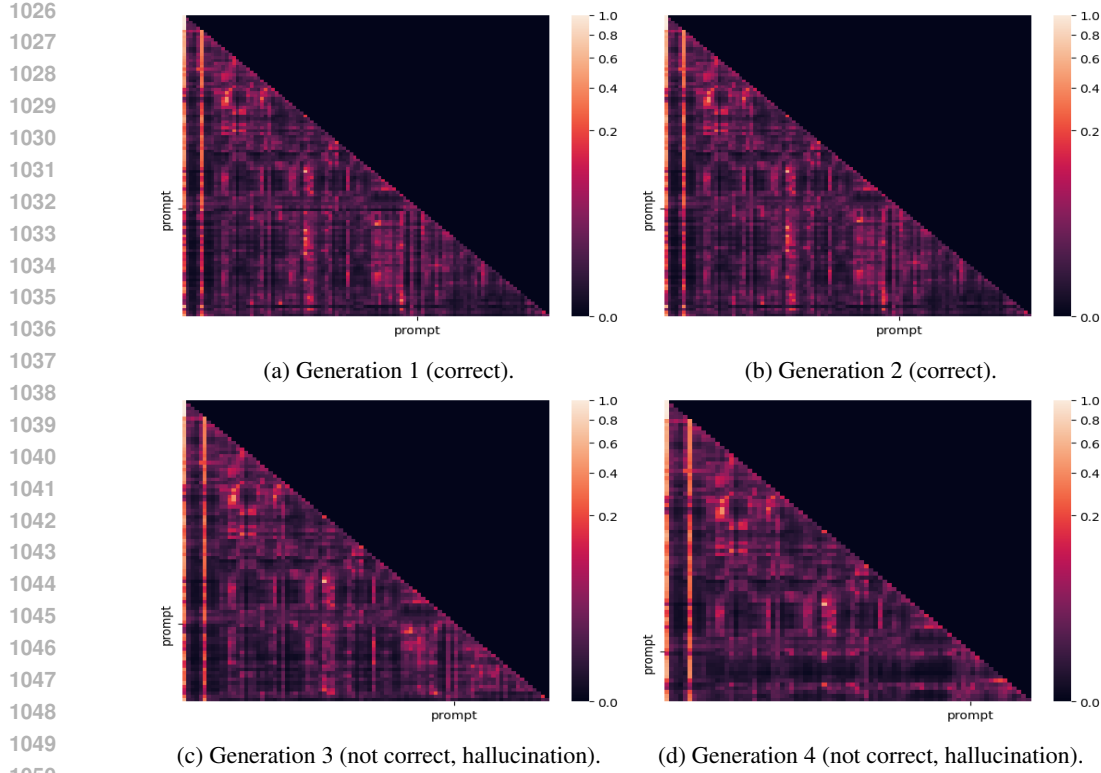


Figure 14: Attention maps. CodeLLama-7B, HumanEval dataset, problem 14, layer 15, head 5.

XGboost classifier using these features. The quality of hallucination detection via such zero-shot prompting is in Table 10, row “DeepSeek R1, (671B model)”. The quality of the proposed approach is shown in Table 10, row “Attn. Feat (ours, from 6.7B model)”. Note that in this case, we use *only* the attention features of the DeepSeek-6.7B model obtained during code generation. Finally, we combine both types of features to train a classifier and report its performance in Table 10, row “Attn. Feat. (ours, from 6.7B model) + DeepSeek R1”. The larger DeepSeek R1 model demonstrates better performance than the classifier trained on attention features. However, by adding an output of DeepSeek R1 to our attention-based features and training the XGBoost classifier, we can achieve the best ROC-AUC score. The study of DeepSeek R1’s Chain of Thoughts shows that this LLM is doing verification of code by interpreting Python code step by step for unit tests. This can explain the high accuracy of Deep Seek R1. At the same time, our method opens opportunities for a deeper understanding of inner working and information flow inside transformer models. Our attention features were based on a small 6.7B model in this experiment, however, our features were able to improve the performance of DeepSeek R1.

Additionally, we performed a similar experiment with QwenCoder2.5-32B. In this case, we use the same QwenCoder2.5-32B to generate code, extract attention features, and evaluate its performance with zero-shot prompting. Table 11 provides the experimental results. The proposed approach is capable of achieving a better detection quality than zero-shot the prompting, which supports the applicability of the proposed approach to larger models.

Furthermore, we provide a comparison with CODEJUDGE Tong & Zhang (2024), a code evaluation framework that uses LLM to analyze code functionality and then decide on code correctness. In our comparison, we use CodeLLama-Instruct 34B as an evaluation model to produce binary output to show whether the generated code is correct or not. We report the mean results over 3 runs in accordance with the original setup; see Tables 13, 14, 15.

We highlight that for a fair comparison we should consider the setup when CODEJUDGE is run without reference and Attn. Feat. is run for large 32-34B models. In our work, we did not include

1080 Table 6: Ablation study for the choice of a classification model for code hallucination detection.
1081

Model	HumanEval		MBPP	
	ROC-AUC	F1-Score	ROC-AUC	F1-Score
StarCoder2-7B				
XGBoost	82.9 \pm 2.7	54.2 \pm 6.9	81.9 \pm 2.4	68.4 \pm 5.3
MLP	80.9 \pm 4.7	60.7 \pm 7.6	81.1 \pm 1.7	68.7 \pm 3.0
Logistic Regression	84.3 \pm 3.9	64.2 \pm 8.0	82.9 \pm 2.3	69.7 \pm 3.4
SVC	84.9 \pm 4.0	65.6 \pm 7.4	82.3 \pm 2.6	69.1 \pm 4.4
CodeLlama-7B				
XGBoost	85.6 \pm 3.9	56.4 \pm 7.2	83.4 \pm 3.3	64.0 \pm 4.4
MLP	81.8 \pm 7.2	58.1 \pm 11.8	81.6 \pm 2.2	64.4 \pm 5.6
Logistic Regression	81.8 \pm 7.1	58.2 \pm 7.9	82.6 \pm 2.1	63.6 \pm 4.7
SVC	83.2 \pm 5.4	59.8 \pm 9.2	82.4 \pm 1.2	60.9 \pm 4.6
DeepSeek-Coder-6.7B				
XGBoost	85.6 \pm 2.8	68.9 \pm 5.5	82.6 \pm 1.9	76.5 \pm 2.7
MLP	84.3 \pm 2.4	69.6 \pm 3.9	81.7 \pm 1.1	74.8 \pm 1.9
Logistic Regression	85.8 \pm 3.2	71.1 \pm 4.7	81.8 \pm 2.4	75.7 \pm 2.2
SVC	87.0 \pm 2.4	72.9 \pm 3.7	81.4 \pm 1.6	75.2 \pm 1.7
Qwen2.5-Coder-7B				
XGBoost	81.7 \pm 2.8	70.2 \pm 4.2	82.2 \pm 2.2	75.4 \pm 1.7
MLP	81.3 \pm 1.6	70.8 \pm 2.5	79.5 \pm 2.0	72.9 \pm 3.0
Logistic Regression	80.0 \pm 1.6	71.3 \pm 3.8	81.0 \pm 1.9	75.9 \pm 2.0
SVC	79.6 \pm 1.7	68.9 \pm 2.4	81.0 \pm 1.7	76.7 \pm 3.3
Magicoder-S-DS-6.7B				
XGBoost	82.3 \pm 4.9	80.7 \pm 3.6	77.8 \pm 2.5	73.4 \pm 3.4
MLP	76.5 \pm 3.3	78.9 \pm 1.8	78.6 \pm 3.6	73.3 \pm 3.5
Logistic Regression	81.7 \pm 1.6	81.6 \pm 2.4	81.3 \pm 2.8	82.1 \pm 1.7
SVC	80.5 \pm 2.4	82.0 \pm 3.1	82.5 \pm 2.6	81.3 \pm 1.9

1109
1110 Table 7: HumanEval and MBPP features ablation for smaller models.
1111

Model	HumanEval		MBPP	
	ROC-AUC	F1-Score	ROC-AUC	F1-Score
QwenCoder2.5-1.5b				
Attn. Feat. (ours)	85.9 \pm 4.1	58.1 \pm 9.6	82.8 \pm 1.4	59.2 \pm 2.7
- w/o Diag. Feat.	85.0 \pm 3.8	57.6 \pm 6.8	82.1 \pm 1.8	58.6 \pm 4.2
- w/o MTD Feat.	82.9 \pm 3.9	53.6 \pm 10.8	79.5 \pm 1.5	57.0 \pm 4.5
QwenCoder2.5-3b				
Attn. Feat. (ours)	80.4 \pm 6.6	65.5 \pm 8.5	78.0 \pm 3.0	73.3 \pm 3.6
- w/o Diag. Feat.	79.0 \pm 6.1	67.2 \pm 6.4	79.6 \pm 3.0	74.8 \pm 3.9
- w/o MTD Feat.	74.9 \pm 4.4	59.0 \pm 5.7	75.5 \pm 2.2	71.0 \pm 3.1

1123
1124
1125
1126 reference (i.e. correct solution) to the prompt as this setup is not practical (typically, one does not
1127 know the correct solution). Also, since CODEJUDGE is evaluated with a 34B model, we evaluate
1128 the Attn. Feat. in a similar way to keep the experimental design of both methods as close as pos-
1129 sible. In this comparison, Attn. Feat. outperforms CODEJUDGE in the majority of cases, winning
1130 by a large margin for ROC-AUC. However, to further explore the capabilities of the proposed Attn.
1131 Feat., we provide additional comparison when CODEJUDGE is run with reference and when Attn.
1132 Feat. is run for smaller 6.7-7B models. In these cases, Attn. Feat. still outperforms CODEJUDGE as
1133 measured by ROC-AUC although the F1-score performance is lower in some cases.

1134
1135
1136 Table 8: MBPP transferability ablation.
1137
1138
1139
1140
1141
1142
1143

Method	DeepSeek-Coder-6.7b	QwenCoder2.5-3b	StarCoder2-7b
Attn. Feat. (ours)	72.4	65.6	67.2
- w/o Diag. Feat.	71.3	67.4	64.2
- w/o MTD Feat.	63.5	61.3	66.8

1144
1145
1146
1147
1148
1149
1150
1151
1152
1153
1154
1155
1156
1157
1158
1159
1160
1161
1162
1163
1164
1165
1166
1167
1168
1169
1170
1171
1172
1173
1174
1175
1176
1177
1178
1179
1180
1181
1182
1183
1184
1185
1186
1187
Table 9: HumanEval and MBPP features ablation

Model	HumanEval		MBPP	
	ROC-AUC	F1-Score	ROC-AUC	F1-Score
StarCoder2-7B				
Attn. Feat. (ours)	82.9 ± 2.7	54.2 ± 6.9	81.9 ± 2.4	68.4 ± 5.3
- w/o Diag. Feat.	82.2 ± 4.5	56.1 ± 9.7	80.5 ± 2.8	66.3 ± 5.3
- w/o MTD Feat.	83.8 ± 2.7	52.5 ± 8.4	81.1 ± 2.6	67.7 ± 5.0
CodeLlama-7B				
Attn. Feat. (ours)	85.6 ± 3.9	56.4 ± 7.2	83.4 ± 2.2	64.0 ± 4.4
- w/o Diag. Feat.	83.5 ± 4.8	50.0 ± 6.5	81.5 ± 2.6	60.2 ± 4.2
- w/o MTD Feat.	85.5 ± 4.4	58.3 ± 10.1	83.5 ± 1.8	63.9 ± 4.3
DeepSeek-Coder-6.7B				
Attn. Feat. (ours)	85.6 ± 2.8	68.9 ± 5.5	82.6 ± 1.9	76.5 ± 2.7
- w/o Diag. Feat.	85.1 ± 2.2	67.0 ± 5.9	81.3 ± 2.6	74.9 ± 3.2
- w/o MTD Feat.	84.4 ± 2.2	67.1 ± 3.8	82.2 ± 1.7	75.9 ± 1.7
Qwen2.5-Coder-7B				
Attn. Feat. (ours)	81.7 ± 2.8	70.2 ± 4.2	82.2 ± 2.2	75.4 ± 1.7
- w/o Diag. Feat.	80.6 ± 2.3	68.9 ± 3.9	80.8 ± 2.1	75.4 ± 0.4
- w/o MTD Feat.	78.9 ± 1.9	66.4 ± 1.4	76.9 ± 2.2	71.6 ± 1.7
Magicoder-S-DS-6.7B				
Attn. Feat. (ours)	82.3 ± 4.9	80.7 ± 3.6	81.5 ± 1.6	80.6 ± 2.0
- w/o Diag. Feat.	79.8 ± 2.7	81.1 ± 1.8	81.2 ± 1.9	80.1 ± 1.4
- w/o MTD Feat.	82.1 ± 3.4	81.6 ± 2.6	80.3 ± 2.5	79.7 ± 2.2

K ADDITIONAL RESULTS ON CONTRIBUTION OF INDIVIDUAL HEADS

We carry out additional experiments with 7B-models and MultiPL-E benchmark⁹, which is a translation of HumanEval to several popular programming languages; we used Go, Java, Rust, Lua among them. We find that features of some heads have quite a high correlation with the target value (presence of a hallucination) and can be used as individual predictors. In Table 17 we report the ROC-AUC scores of the top-performing features.

L EVALUATION WITH GREEDY DECODING

In the main experiments in Section 5.2, we use sampling with temperature 0.8 to generate diverse solutions for each coding problem and obtain a larger train and test samples. However, production systems typically use greedy decoding, and in this section we fill this gap. We evaluate the performance of the proposed Attn. Feat. classifier when both train and test data are generated via greedy decoding. In this setup, the sample sizes are 164 for HumanEval and 500 for MBPP with 1 generation per task, and we use cross-validation with 5 folds. Although the sample size is sufficiently smaller than in Section 5.2, the proposed classifier achieves high performance across all models and datasets and can be applied to small size samples; see Table 21.

⁹<https://github.com/nuprl/MultiPL-E>

1188

Table 10: MBPP features for larger models. See Section J for details.

1189

1190

Method	ROC-AUC
DeepSeek-Coder-6.7B	
Attn. Feat (ours, from 6.7B model)	82.6 ± 1.9
DeepSeek R1 (671B model)	92.3 ± 1.1
Attn. Feat. (from 6.7B model) + DeepSeek R1 (671B)	95.1 ± 0.7

1195

1196

1197

Table 11: HumanEval features for larger models. See Section J for details.

1198

1199

1200

1201

1202

1203

1204

1205

M CROSS-MODEL TRANSFERABILITY

1206

In this section, we verify whether the proposed XGBoost classifier trained on the attention features of one model can be effectively applied to detect hallucinations using the attention features of another model. A formal requirement is that the number of attention features of the two models should be the same. The results of cross-model transferability are shown in Tables 22, 23. We conclude that a classifier trained on DeepSeek-Coder-6.7B is transferable to Magicoder-S-DS-6.7B and vice versa, which is not the case for CodeLlama-7B. We suppose the reason is that Magicoder-S-DS-6.7B is a fine-tuned DeepSeek-Coder-6.7B and a correspondence between attention heads persists.

1214

1215

N FAILURE CASE STUDY

1216

We provide a failure case study in the Table 24. For each trained classifier, we analyze the category of generated code which was classified incorrectly by the classifier. We report the fraction of top-3 most popular code categories w.r.t. number of samples in the test sample. We use 5-fold stratified group cross validation and report the average values over 5 folds. The table reveals the most popular failure cases: misclassification of correct codes that passed the tests (referred to as ‘passed’) and misclassification of wrong solutions (i.e. codes that did not pass any test and caused an `AssertionError`). The fraction of other errors (top-3 and others) is sufficiently lower.

1224

1225

1226

1227

1228

1229

1230

1231

1232

1233

1234

1235

1236

1237

1238

1239

1240

1241

1242
 1243
 1244 Table 12: Code hallucination detection for HumanEval dataset for larger models. For each task, 10
 1245 candidate solutions were generated. **Bold** and underline denote the first and second best results.
 1246

Method	ROC-AUC	F1-Score
CodeLlama-34B		
Prompt Len.	57.3 ± 6.3	37.7 ± 13.6
Gen. Len.	62.8 ± 1.8	38.2 ± 4.0
Mean Log. Prob.	74.1 ± 5.0	51.8 ± 7.6
CodeT5-base ft.	54.7 ± 5.5	0.0 ± 0.0
Attn. Feat. (ours)	83.2 ± 3.8	62.5 ± 7.1
All. Feat.	84.8 ± 2.8	62.8 ± 6.7
Qwen2.5-Coder-32B		
Prompt Len.	53.2 ± 9.2	53.4 ± 12.8
Gen. Len.	58.0 ± 3.1	62.5 ± 3.8
Mean Log. Prob.	65.8 ± 4.8	63.6 ± 2.8
CodeT5-base ft.	53.3 ± 4.5	59.5 ± 15.2
Attn. Feat. (ours)	85.0 ± 2.7	<u>77.0 ± 5.5</u>
All. Feat.	84.9 ± 3.1	77.7 ± 5.7
DeepSeek-Coder-33B		
Prompt Len.	53.3 ± 6.5	44.0 ± 5.3
Gen. Len.	56.6 ± 4.2	48.2 ± 3.4
Mean Log. Prob.	66.4 ± 3.4	57.1 ± 2.9
CodeT5-base ft.	57.6 ± 3.9	1.1 ± 2.2
Attn. Feat. (ours)	<u>88.0 ± 2.9</u>	<u>77.9 ± 2.2</u>
All. Feat.	88.9 ± 2.8	78.6 ± 3.1

1271 Table 13: Additional comparison with CODEJUDGE Tong & Zhang (2024) on HumanEval for 32-
 1272 34B models.
 1273

Method	CodeLlama-34B		DeepSeek-Coder-33B		Qwen2.5-Coder-32B	
	ROC-AUC	F1-Score	ROC-AUC	F1-Score	ROC-AUC	F1-Score
CODEJUDGE						
A.S. w/o reference	65.3 ± 3.0	69.6 ± 4.8	72.0 ± 7.2	80.2 ± 3.8	61.6 ± 7.3	81.8 ± 4.7
CODEJUDGE						
A.S. w/ reference	68.7 ± 3.8	70.0 ± 5.4	75.8 ± 5.6	81.1 ± 2.4	62.0 ± 7.5	80.3 ± 2.0
Attn. Feat.	75.0 ± 5.1	68.4 ± 5.9	86.5 ± 7.2	81.6 ± 4.0	74.0 ± 6.4	82.7 ± 1.6

1281
 1282
 1283
 1284 Table 14: Additional comparison with CODEJUDGE Tong & Zhang (2024) on HumanEval for Star-
 1285 Coder2-7B, CodeLlama-7B, DeepSeekCoder-6.7B.
 1286

Method	StarCoder2-7B		CodeLlama-7B		DeepSeekCoder-6.7b	
	ROC-AUC	F1-Score	ROC-AUC	F1-Score	ROC-AUC	F1-Score
CODEJUDGE						
A.S. w/o reference	70.6 ± 4.7	64.8 ± 4.3	71.3 ± 4.1	59.2 ± 3.8	69.2 ± 3.2	74.4 ± 4.8
CODEJUDGE						
A.S. w/ reference	75.8 ± 4.7	68.2 ± 3.9	73.0 ± 3.3	61.0 ± 5.3	68.8 ± 7.9	70.9 ± 9.0
Attn. Feat.	80.8 ± 3.7	63.5 ± 9.1	80.1 ± 3.9	59.9 ± 9.4	83.9 ± 8.4	78.5 ± 6.7

1296
 1297 Table 15: Additional comparison with CODEJUDGE Tong & Zhang (2024) on HumanEval for
 1298 QwenCoder-7B, Magicoder-S-DS-6.7B.
 1299

1300 Method	1301 QwenCoder-7b		1302 Magicoder-S-DS-6.7b	
	1303 ROC-AUC	1304 F1-Score	1305 ROC-AUC	1306 F1-Score
1307 CODEJUDGE A.S. w/o reference	1308 67.2 ± 5.7	1309 78.1 ± 3.5	1310 55.3 ± 2.7	1311 83.3 ± 6.6
1312 CODEJUDGE A.S. w/ reference	1313 70.4 ± 7.4	1314 77.6 ± 4.3	1315 57.9 ± 7.1	1316 82.1 ± 3.6
1317 Attn. Feat.	1318 73.3 ± 7.1	1319 73.7 ± 6.1	1320 65.1 ± 3.4	1321 85.4 ± 5.4

1305
 1306 Table 16: Code hallucination detection with attention features for MBPP dataset with increasing
 1307 complexity of prompt: two-shot prompts.
 1308

1309 Method	1310 ROC-AUC	1311 F1-Score
	1312 Qwen2.5-Coder-7B	
Prompt Len.	53.5 ± 2.9	60.2 ± 1.5
Gen. Len.	56.9 ± 3.3	63.2 ± 2.0
Mean Log. Prob.	58.1 ± 2.6	61.1 ± 3.3
Attn. Feat. (ours)	78.3 ± 3.1	74.2 ± 1.8
All. Feat.	76.7 ± 2.7	72.2 ± 2.1
Self-Eval	68.4 ± 1.0	77.4 ± 2.4
Interrogate-LLM	56.6 ± 1.5	69.1 ± 2.1
1318 DeepSeek-Coder-6.7B		
Prompt Len.	56.0 ± 2.0	58.0 ± 2.4
Gen. Len.	54.4 ± 1.3	59.6 ± 1.6
Mean Log. Prob.	64.9 ± 1.7	64.2 ± 2.4
Attn. Feat. (ours)	81.4 ± 2.2	75.0 ± 5.3
All. Feat.	80.4 ± 0.7	74.5 ± 2.6
Self-Eval	50.0 ± 0.0	69.3 ± 5.1
Interrogate-LLM	61.1 ± 3.1	69.4 ± 5.2

1326
 1327 Table 17: ROC AUC scores of top-performing features across several benchmarks.
 1328

1329 Feature	1330 HumalEval					1331 MBPP
	1332 Python	1333 Go	1334 Rust	1335 Java	1336 Lua	1337 Python
StarCoder2-7B						
avg. prompt's self-attention, layer 14, head 0	70.8	76.8	74.6	68.9	70.3	55.2
avg. prompt's self-attention, layer 15, head 5	71.1	78.4	75.1	72.9	72.4	58.1
avg. prompt's self-attention, layer 23, head 20	69.2	72.2	74.2	64.7	67.7	50.7
CodeLlama-7B						
-MTD ₁ (P, G)/ P , layer 15, head 27	67.6	71.1	73.7	71.0	–	66.1
avg. prompt's self-attention, layer 7, head 22	74.6	75.7	76.5	69.7	–	63.1
MTD ₀ (P, G)/ P , layer 11, head 23	69.1	71.0	71.9	65.4	–	69.1
DeepSeek-Coder-6.7B						
MTD ₀ (P, G)/ P , layer 30, head 11	67.5	65.7	67.0	66.3	69.1	58.1
avg. prompt's self-attention, layer 12, head 17	65.0	73.6	70.0	69.8	69.8	58.2
avg. prompt's self-attention, layer 12, head 23	64.1	71.0	66.8	64.4	67.6	58.2
Qwen2.5-Coder-7B						
avg. generation's self-attention, layer 24, head 2	65.8	60.2	58.8	60.2	66.7	60.8
MTD ₀ (P, G)/ P , layer 11, head 5	66.2	68.8	59.5	61.6	72.7	59.4
avg. prompt's self-attention, layer 9, head 26	65.4	75.8	66.9	67.0	71.1	61.0
Magicoder-S-DS-6.7B						
MTD ₀ (P, G)/ P , layer 30, head 11	68.8	70.2	60.0	65.1	63.8	58.2
avg. prompt's self-attention, layer 13, head 13	63.1	64.9	69.0	67.3	63.2	58.8
avg. prompt's self-attention, layer 12, head 17	63.0	63.2	68.0	67.1	60.8	58.9

1350

1351 Table 18: Characteristics of generated data, Pass@1. For each problem, we generated 25 candidate
1352 solutions for HumanEval, Python, 10 candidate solutions for HumanEval, Java, Go, Rust, Lua, and
1353 5 candidate solutions for MBPP.

1354

Model	HumalEval					MBPP
	Python	Java	Go	Rust	Lua	
StarCoder2-7B	28.9	24.5	17.5	20.9	19.1	42.8
CodeLlama-7B	25.9	25.8	17.6	20.8	0.0	35.2
DeepSeek-Coder-6.7B	40.3	33.5	23.6	28.7	16.6	52.6
Qwen2.5-Coder-7B	47.8	22.7	11.9	22.6	23.5	52.1
Magicoder-S-DS-6.7B	65.5	48.9	40.3	44.2	34.6	61.3

1361

1362

1363

1364 Table 19: Performance of the proposed method on different programming languages, ROC-AUC.

1365

Model	Java	Go	Rust	Lua
StarCoder2-7B	82.7 ± 4.9	86.5 ± 3.6	82.4 ± 5.2	82.0 ± 3.5
CodeLlama-7B	76.8 ± 6.1	81.9 ± 6.2	77.5 ± 10.8	–
DeepSeek-Coder-6.7B	84.9 ± 4.2	84.7 ± 2.9	82.8 ± 7.1	86.7 ± 4.3
Qwen2.5-Coder-7B	82.6 ± 4.1	91.8 ± 0.9	87.3 ± 2.6	90.2 ± 3.0
Magicoder-S-DS-6.7B	77.8 ± 4.5	80.8 ± 2.0	75.1 ± 5.9	79.0 ± 3.2

1371

1372

1373

1374 Table 20: Performance of the proposed method on different programming languages, F1-Score.

1375

Model	Java	Go	Rust	Lua
StarCoder2-7B	50.4 ± 7.6	39.7 ± 11.9	36.5 ± 9.2	39.0 ± 8.7
CodeLlama-7B	36.4 ± 20.6	26.5 ± 10.2	34.8 ± 17.3	–
DeepSeek-Coder-6.7B	64.1 ± 4.5	53.2 ± 8.7	56.8 ± 6.6	41.6 ± 15.1
Qwen2.5-Coder-7B	45.8 ± 9.6	37.6 ± 11.5	49.9 ± 6.9	64.6 ± 7.9
Magicoder-S-DS-6.7B	68.0 ± 4.9	63.3 ± 2.0	63.1 ± 8.7	58.4 ± 6.7

1381

1382

1383 Table 21: Quality of code hallucination detection for HumanEval and MBPP datasets when greedy
1384 decoding is used to generate candidate solutions.

1385

Model	HumalEval		MBPP	
	ROC-AUC	F1-Score	ROC-AUC	F1-Score
StarCoder2-7B	80.8 ± 3.7	61.9 ± 9.5	79.3 ± 6.1	69.7 ± 5.4
CodeLlama-7B	80.1 ± 3.9	59.4 ± 10.0	82.3 ± 3.1	71.3 ± 6.3
DeepSeek-Coder-6.7B	83.9 ± 8.4	78.5 ± 6.7	79.6 ± 3.4	78.7 ± 2.1
Qwen2.5-Coder-7B	73.3 ± 7.1	70.1 ± 6.4	74.0 ± 1.9	75.7 ± 4.0
Magicoder-S-DS-6.7B	65.1 ± 3.4	82.6 ± 4.3	79.3 ± 2.0	80.8 ± 1.3

1393

1394

1395 Table 22: Quality of code hallucination detection in cross-model transferability on HumanEval.
1396 Rows correspond to train and columns correspond to test samples.

1397

Test	CodeLlama-7B		DeepSeek-Coder-6.7B		Magicoder-S-DS-6.7B	
	ROC-AUC	F1-Score	ROC-AUC	F1-Score	ROC-AUC	F1-Score
Train						
CodeLlama-7B	85.6 ± 3.9	56.4 ± 7.2	51.9 ± 13.2	17.3 ± 21.1	51.1 ± 7.1	24.3 ± 29.0
DeepSeek-Coder-6.7B	45.4 ± 10.3	14.2 ± 9.6	85.6 ± 2.8	68.9 ± 5.5	79.4 ± 3.7	69.4 ± 6.8
Magicoder-S-DS-6.7B	51.8 ± 5.4	23.4 ± 17.7	83.0 ± 2.2	70.7 ± 2.7	82.3 ± 4.9	80.7 ± 3.6

1403

1404

1405

1406

1407

1408

1409

1410

1411

1412

1413 Table 23: Quality of code hallucination detection in cross-model transferability on MBPP. Rows
1414 correspond to train and columns correspond test samples.

1415

1416

Test	CodeLlama-7B		DeepSeek-Coder-6.7B		Magicoder-S-DS-6.7B	
Train	ROC-AUC	F1-Score	ROC-AUC	F1-Score	ROC-AUC	F1-Score
CodeLlama-7B	83.4 ± 3.3	64.0 ± 4.4	49.3 ± 2.9	17.2 ± 22.6	52.3 ± 9.4	21.9 ± 26.8
DeepSeek-Coder-6.7B	49.2 ± 5.5	21.0 ± 17.8	82.6 ± 1.9	76.5 ± 2.7	75.2 ± 1.6	54.5 ± 11.3
Magicoder-S-DS-6.7B	51.8 ± 3.4	29.2 ± 24.0	64.8 ± 6.4	58.5 ± 13.9	81.5 ± 1.6	80.6 ± 2.0

1421

1422

1423

1424

1425

1426

1427

1428

1429

1430

1431

1432

1433

1434

1435

1436

1437

1438

1439

1440 Table 24: Failure case study. “P” - Passed, “AE” - AssertionError, “NE” - NameError, “IE” - Index-
1441 Error, “TE” - TypeError.

1442

1443

Model	HumanEval			MBPP		
	Top-1	Top-2	Top-3	Top-1	Top-2	Top-3
StarCoder2-7b	P 17.2 ± 4.5	AE 2.9 ± 2.2	NE 0.8 ± 0.5	P 15.0 ± 3.5	AE 9.7 ± 2.2	NE 0.7 ± 0.4
CodeLLama-7b	P 14.6 ± 3.6	AE 3.8 ± 2.7	NE 0.2 ± 0.2	P 15.5 ± 1.6	AE 7.4 ± 1.2	NE 0.5 ± 0.4
DeepSeekCoder-6.7b	P 14.6 ± 2.9	AE 4.9 ± 1.2	IE 0.5 ± 0.6	AE 12.6 ± 3.2	P 11.1 ± 3.8	NE 0.7 ± 0.5
QwenCoder-7b	P 16.0 ± 5.4	AE 6.9 ± 2.8	NE 2.1 ± 0.7	P 11.3 ± 0.5	AE 10.8 ± 1.4	NE 1.3 ± 0.5
Magicoder-6.7b	AE 12.1 ± 4.8	P 10.4 ± 4.8	IE 0.7 ± 0.6	AE 14.5 ± 4.4	P 9.2 ± 2.3	TE 0.6 ± 0.5

1449

1450

1451

1452

1453

1454

1455

1456

1457